Prog. Theor. Exp. Phys. **2022** 043B01(40 pages)
DOI: 10.1093/ptep/ptac018

Supersymmetric gauge theory on the graph

So Matsuura[1] and Kazutoshi Ohta[2,⋆]

[1] *Hiyoshi Departments of Physics, and Research and Education Center for Natural Sciences, Keio University, 4-1-1 Hiyoshi, Yokohama, Kanagawa 223-8521, Japan*
[2] *Institute of Physics, Meiji Gakuin University, Yokohama, Kanagawa 244-8539, Japan*
⋆E-mail: kohta@law.meijigakuin.ac.jp

Received November 16, 2021; Revised December 30, 2021; Accepted January 26, 2022; Published January 28, 2022

We consider two-dimensional $\mathcal{N} = (2, 2)$ supersymmetric gauge theory on discretized Riemann surfaces. We find that the discretized theory can be efficiently described by using graph theory, where the bosonic and fermionic fields are regarded as vectors on a graph and its dual. We first analyze the Abelian theory and identify its spectrum in terms of graph theory. In particular, we show that the fermions have zero modes corresponding to the topology of the graph, which can be understood as kernels of the incidence matrices of the graph and the dual graph. In the continuous theory, a scalar curvature appears as an anomaly in the Ward–Takahashi identity associated with a $U(1)$ symmetry. We find that the same anomaly arises as the deficit angle at each vertex on the graph. By using the localization method, we show that the path integral on the graph reduces to an integral over a set of the zero modes. The partition function is then ill-defined unless suitable operators are inserted. We extend the same argument to the non-Abelian theory and show that the path integral reduces to multiple integrals of Abelian theories at the localization fixed points.

Subject Index B16, B27, B31, B38

1. Introduction

Gauge theory has been recognized as the most fundamental theory describing the interaction of elementary particles. However, in recent years, the importance of gauge theory has been extended and it has come to be recognized as a powerful tool for approaching the quantum theory of gravity through the gauge/gravity duality [1–3]. In particular, the gauge/gravity duality predicted by superstring theory provides a clear dictionary between the gauge and gravity theories with supersymmetry. Since supersymmetric gauge theories can give mathematically accurate descriptions for some physical quantities by using strong constraints based on supersymmetry, they have traditionally been studied in analytic ways. However, the prediction of the gauge/gravity duality should also be applied to dynamical quantities. To approach quantum gravity through supersymmetric gauge theories, therefore, we need to have the means to analyze their dynamics in a non-perturbative way.

One of the most effective non-perturbative approaches to gauge theories is lattice gauge theory, which regularizes gauge field theory on a finite lattice and defines the continuous theory as the continuum limit of the discretized theory. Various attempts have been made to construct lattice gauge theories that preserve some of the supersymmetries on the square lattice [4–22]. The relations between these models were investigated in Refs. [23–27], and several numerical computations based on these models have been carried out [28–42]. In two dimensions, the theory is super renormalizable, and numerical calculations can be performed without maintaining supersymmetry with a small number of fine-tunings [29]. In Ref. [43], two-dimensional $\mathcal{N} = (2, 2)$ supersymmetric $SU(2)$ Yang–Mills theory was investigated numerically using a lattice theory with a conventional Wilson fermion. For reviews, see Refs. [44–49].

Among these lattice theories, the models constructed by Sugino (Sugino models) [4–8] have the gauge group $SU(N)$, while the gauge group of the other models is inevitably $U(N)$. As a result, the link variables in the Sugino models are expressed by compact unitary matrices as in conventional lattice gauge theories. In the Sugino models, the action is written by an exact form of scalar supercharges constructed by topological twisting. These scalar supersymmetries are then manifestly preserved even if the translational symmetry is explicitly broken by the discretization of space-time. The problem of vacuum degeneracy of a lattice gauge field has been solved without using an admissibility condition [50], and tree-level improvement has been proposed [51].

In Ref. [52], the Sugino model defined on the usual square lattice was extended to a theory on a discrete space-time where the two-dimensional Riemann surface is divided by polygons. This model (the generalized Sugino model) has been subjected to rigorous analysis using the method of localization [53] and numerical calculations [54].

In this paper, we reconstruct and analyze the generalized Sugino model in two-dimensional supersymmetric gauge theories by using graph theory. (For an introduction to graph theory, see, e.g., Ref. [55].) We regard the vertices and edges of the polygons on the discretized Riemann surface as a graph. We assume that the graph is a directed graph with an edge orientation. We also assume that faces are assigned to the vertices of the dual graph. The directed graph can introduce a “difference” between adjacent vertices, and the difference operator expressed by a matrix is called an incidence matrix. Using this incidence matrix, it is possible to construct a field theory on the discrete space-time represented by the graph, including supersymmetry.

The generalized Sugino model has been analyzed using the method of localization owing to supersymmetry in Ref. [53], but the use of graph theory makes it possible to discuss things more clearly. In particular, we can see the structure of the zero modes, which play an important role in the localization. The zero modes appear as a kernel of the incidence matrix in the context of graph theory, and thus we can use linear algebra to understand their properties. In addition, analysis by graph theory is also beneficial in understanding the anomaly since the zero modes are important in understanding the anomaly of the theory even in the discretized theory. For analysis of field theories and quantum mechanics on the graph, including supersymmetry from other viewpoints, see Refs. [56–58]. See also Ref. [59] for localization in the quiver gauge theory using the technology of graph theory.

The organization of this paper is as follows. In Sect. 2 we briefly review the construction of $\mathcal{N} = (2, 2)$ supersymmetric Yang–Mills theory on the smooth Riemann surface by using differential forms. The formulation with differential forms makes the relation to the graph structure clearer later. We also derive the currents and the Ward–Takahashi (WT) identities corresponding to the global symmetry of the theory. In Sect. 3 we prepare some basics of graph theory for the discretization of the Riemann surface. We also introduce some useful matrices, including the incidence matrix, and summarize their properties in graph theory. In Sect. 4 we formulate a supersymmetric Abelian gauge theory using graph theory and discuss the properties of the fermion zero modes. We derive the chiral anomaly on the graph and show that the fermion zero modes play an important role. We see that the anomaly in the WT identity, which appears as the scalar curvature in the continuous theory, appears as the deficit angle in the theory on the graph. In Sect. 5 we perform the path integral for the Abelian theory using the localization method. We see that a residual integral exists over the zero modes after integrating out the non-zero modes. The integral over the zero modes makes the partition function itself ill-defined, but we also discuss a remedy for this problem by inserting operators including bi-linear terms of the fermions. In Sect. 6 we generalize the localization arguments to non-Abelian theory. By the saddle point approximation in the localization method, non-zero modes give a Vandermonde-type measure and the path integral reduces to multiple integrals of the Abelian theory one. We see that the zero modes play an important role for the non-Abelian as well as the Abelian theory. Section 7 is devoted to conclusions and discussion. In the appendix we give some concrete examples of the graph structure and properties of the incidence matrix and Laplacian. We also give the convention of Weyl–Cartan bases, which are used for non-Abelian theory.

2. Supersymmetric gauge theory on the Riemann surface

2.1 *Action and currents in supersymmetric gauge theory*

We start with a review of supersymmetric gauge theory on the smooth Riemann surface Σ_h (continuous space-time) with genus (handles) h. The theory considered here is essentially obtained by dimensional reduction from four-dimensional $\mathcal{N} = 1$ supersymmetric gauge theory with four supercharges, namely two-dimensional $\mathcal{N} = (2, 2)$ supersymmetric gauge theory. In general, however, when one simply constructs this theory on a curved manifold, the supersymmetry is completely broken. The point is that part of the supersymmetry can be restored by introducing a specific $U(1)$ gauge field as a background in accordance with the spin connection of the background space-time. The supersymmetric theory obtained by this procedure naturally becomes a topologically twisted theory on the curved space-time, and half of the supersymmetry is recovered in general. Among the possible topological twistings, which depend on how to turn on the background gauge field, we choose the so-called topological A-model throughout this paper. (See also Refs. [59,60] for a more detailed construction.)

Because of the topological twisting, not only the bosonic fields but also the fermion fields have integer spins. It is therefore convenient to express the fields in this theory by differential forms: the 0-form scalar fields are Φ, $\bar{\Phi}$, and η; the 1-form vector fields are $A \equiv A_\mu dx^\mu$ and $\lambda \equiv \lambda_\mu dx^\mu$; and the 2-form fields are $Y \equiv \frac{1}{2} Y_{\mu\nu} dx^\mu \wedge dx^\nu$ and $\chi \equiv \frac{1}{2}\chi_{\mu\nu} dx^\mu \wedge dx^\nu$, where Φ, $\bar{\Phi}$, A, and Y are bosons, and η, λ, and χ are fermions (Grassmann valued).

We write Q for one of the supercharges, which transforms the fields as[1]

$$
\begin{aligned}
&Q\Phi = 0, && \\
&Q\bar{\Phi} = 2\eta, && Q\eta = \tfrac{i}{2}[\Phi, \bar{\Phi}], \\
&QA = \lambda, && Q\lambda = -d_A\Phi, \\
&QY = i[\Phi, \chi], && Q\chi = Y,
\end{aligned}
\tag{1}
$$

where $d_A\Phi \equiv d\Phi + i[A, \Phi]$ is a covariant exterior derivative for the adjoint scalar field. We can see that the square of Q generates the gauge transformation with a parameter Φ, which is denoted by $Q^2 = \delta_\Phi$.

Using this supercharge, we can write the action of the theory in Q-exact form:

$$
S = -\frac{1}{2g^2} Q \int_{\Sigma_h} \mathrm{Tr}\left\{\frac{i}{2}\eta[\Phi, \bar{\Phi}]\omega + d_A\bar{\Phi} \wedge *\lambda + \chi *(Y - 2F)\right\},
\tag{2}
$$

[1]The notation of the Q transformation has been slightly changed from Refs. [52–54].

where ω is a volume (Kähler) form on Σ_h, $*$ represents the Hodge star operation which maps from an n-form to a $(2-n)$-form, and

$$F \equiv dA + iA \wedge A \tag{3}$$

is a field strength, which will give a kinetic term of the gauge field after integrating out the auxiliary field Y.

More concretely, after applying the Q transformation, the bosonic and fermionic parts of the action are given by

$$S_{\mathrm{B}} = \frac{1}{2g^2}\int_{\Sigma_h} \mathrm{Tr}\left\{\frac{1}{4}[\Phi, \bar{\Phi}]^2\omega + d_A\bar{\Phi}\wedge * d_A\Phi - Y*(Y-2F)\right\}, \tag{4}$$

$$S_{\mathrm{F}} = \frac{1}{2g^2}\int_{\Sigma_h} \mathrm{Tr}\left\{i\eta[\Phi, \eta]\omega + 2\eta d_A*\lambda - i\lambda\wedge*[\bar{\Phi}, \lambda] + i\chi*[\Phi, \chi] - 2\chi*d_A\lambda\right\}, \tag{5}$$

respectively.

For later convenience, we define a vector of fermionic fields in the order

$$\Psi \equiv \begin{pmatrix}\eta\\ \chi\\ \lambda\end{pmatrix}. \tag{6}$$

Then, the fermionic part of the action in Eq. (5) reduces to

$$S_{\mathrm{F}} = \frac{1}{2g^2}\mathrm{Tr}\int_{\Sigma_h} \Psi^{\mathrm{T}} \wedge * \left(i\not{D}_A + \mathcal{M}_\Phi\right)\Psi, \tag{7}$$

where $\not{D}_A$ and $\mathcal{M}_\Phi$ are the Dirac operator and the mass matrix depending on Φ and $\bar{\Phi}$, respectively:

$$\not{D}_A \equiv \begin{pmatrix} 0 & 0 & id_A^\dagger\\ 0 & 0 & id_A\\ -id_A & -id_A^\dagger & 0\end{pmatrix}, \qquad \mathcal{M}_\Phi \equiv \begin{pmatrix} i[\Phi, \cdot] & 0 & 0\\ 0 & i[\bar{\Phi}, \cdot] & 0\\ 0 & 0 & -i[\Phi, \cdot]\end{pmatrix}. \tag{8}$$

Here,

$$d_A^\dagger \equiv - * d_A * \tag{9}$$

is the co-differential operator, which maps from an n-form to an $(n-1)$-form on Σ_h, and $[\Phi, \cdot]$ represents an adjoint action induced by Φ.

Let us now consider yet another supercharge $\tilde{Q}$. Since there are two preserved supercharges on the curved Riemann surface, we have the supercharge $\tilde{Q}$ in addition to Q. The supersymmetry transformation for the vector multiplet is given by

$$\begin{aligned}
&\tilde{Q}\Phi = 0, & &\\
&\tilde{Q}A = *\lambda, & &\tilde{Q}\lambda = *d_A\Phi,\\
&\tilde{Q}\bar{\Phi} = 2*\chi, & &\tilde{Q}\chi = \tfrac{i}{2}[\Phi, \bar{\Phi}]\omega,\\
&\tilde{Q}Y = -i[\Phi, \eta]\omega, & &\tilde{Q}\eta = -*Y.
\end{aligned} \tag{10}$$

Roughly speaking, $\tilde{Q}$ swaps the role of the 0-form η and the 2-form χ against the action of Q. We can also see that the square of $\tilde{Q}$ becomes the gauge transformation, namely $\tilde{Q}^2 = \delta_\Phi$, and Q and $\tilde{Q}$ anti-commute with each other:

$$\{Q, \tilde{Q}\} = 0. \tag{11}$$

Using the transformation of $\tilde{Q}$, we can also write the action in the $\tilde{Q}$-exact form

$$S = -\frac{1}{2g^2}\tilde{Q}\int_{\Sigma_h} \mathrm{Tr}\left\{\frac{i}{2}\chi[\Phi, \bar{\Phi}] + \lambda\wedge d_A\bar{\Phi} - \eta(Y-2F)\right\}, \tag{12}$$

so the action is also invariant under $\tilde{Q}$. This comes from the fact that the action is written by

$$S = \frac{1}{4g^2}[Q, \tilde{Q}] \int_{\Sigma_h} \mathrm{Tr}\left\{\bar{\Phi}F + \eta\chi\right\}. \tag{13}$$

Using also the anti-commuting relation between Q and $\tilde{Q}$, we can find that the action is written in both Q- and $\tilde{Q}$-exact forms. Note also that the part acting the supercharges in Eq. (13) is invariant under swapping (a rotation of) η and χ.

2.2 *Symmetries and relations among conserved currents*

We next consider the global symmetries of this theory and the associated Noether currents. In general, if a theory is invariant under a certain global transformation, the infinitesimal transformation of the action can be written as

$$\delta_\xi S = \xi\, \boldsymbol{s} S = \int_{\Sigma_h} \left(d\xi * \tilde{J}_s + \xi dI_s\right), \tag{14}$$

where $\boldsymbol{s}$ is the generator of this transformation, ξ is a position-dependent parameter, and $\tilde{J}_s$ and I_s are both one-forms. Then, the corresponding Noether current is defined by

$$J_s = \tilde{J}_s + *I_s, \tag{15}$$

which is conserved, at least classically:

$$d^\dagger J_s = 0. \tag{16}$$

Note that this current is invariant if we add any s-invariant total derivative term to the action.

Using this prescription, the Noether current corresponding to the Q and $\tilde{Q}$ symmetries are respectively constructed as

$$J_Q = \frac{1}{g^2}\mathrm{Tr}\left\{d_A\Phi\eta + *d_A\Phi*\chi - \frac{i}{2}[\Phi, \bar{\Phi}]\lambda - *Y*\lambda\right\}, \tag{17}$$

$$J_{\tilde{Q}} = \frac{1}{g^2}\mathrm{Tr}\left\{-*d_A\Phi\eta + d_A\Phi*\chi - \frac{i}{2}[\Phi, \bar{\Phi}]*\lambda + *Y\lambda\right\}. \tag{18}$$

The theory also possesses two global $U(1)$ symmetries, $U(1)_A$ and $U(1)_V$. The $U(1)_A$ symmetry transforms the fields as

$$\delta_A A = 0, \qquad \delta_A\Phi = 2i\theta_A\Phi, \qquad \delta_A\bar{\Phi} = -2i\theta_A\bar{\Phi}, \qquad \delta\Psi = i\theta_A\gamma_A\Psi, \tag{19}$$

where

$$\gamma_A \equiv \begin{pmatrix} -1 & 0 & 0 \\ 0 & -1 & 0 \\ 0 & 0 & 1 \end{pmatrix}, \tag{20}$$

and the $U(1)_V$ symmetry transforms the fields as

$$\delta_V A = 0, \qquad \delta_V\Phi = 0, \qquad \delta_V\bar{\Phi} = 0, \qquad \delta_V\Psi = i\theta_V\gamma_V\Psi, \tag{21}$$

where

$$\gamma_V \equiv -i\begin{pmatrix} 0 & * & 0 \\ -* & 0 & 0 \\ 0 & 0 & * \end{pmatrix}. \tag{22}$$

The corresponding Noether currents are given by

$$J_A = \frac{i}{g^2}\mathrm{Tr}\left(-\bar{\Phi}d_A\Phi + \Phi d_A\bar{\Phi} + \eta\lambda - *\lambda * \chi\right), \tag{23}$$

$$J_V = \frac{1}{g^2}\mathrm{Tr}\,(\eta * \lambda + \lambda * \chi)\,. \tag{24}$$

Note that γ_A and γ_V satisfy $\gamma_A^2 = \gamma_V^2 = 1$. We will soon see that the $U(1)_A$ symmetry is anomalous quantum mechanically.

We point out that there are important relationships among the supercurrents J_Q, $J_{\tilde{Q}}$, and the current J_V [36]:

$$QJ_V = -J_{\tilde{Q}}, \tag{25}$$

$$\tilde{Q}J_V = J_Q. \tag{26}$$

This means that the conservation law of the $U(1)_V$ symmetry guarantees the conservation law of the $\tilde{Q}$ symmetry:

$$d^\dagger J_V = 0 \quad \Rightarrow \quad d^\dagger J_{\tilde{Q}} = 0, \tag{27}$$

if the Q symmetry is preserved.

2.3 *Ward–Takahashi identities and anomaly*

We next consider the WT identities. In the path integral formalism, the WT identity is derived from the obvious invariance under a change of variables,

$$\int dX\, \mathcal{O}(x_0) e^{-S[X]} = \int dX'\, \mathcal{O}'(x_0) e^{-S[X']}, \tag{28}$$

where X expresses the fields of the theory, X' the transformed fields of X,[2] and $\mathcal{O}(x_0)$ is a local operator at a position x_0. Note that this identity can be applied regardless of whether or not the classical action is invariant under the transformation. So, if we consider a general transformation with parameter $\xi(x)$ and generator $\boldsymbol{s}$, the infinitesimal transformations of the action S and the operator $\mathcal{O}$ are given by

$$\delta S = \int_{\Sigma_h} dx\, \xi(x) K_s(x), \tag{29}$$

$$\delta\mathcal{O}(x_0) = \xi(x_0)\, \boldsymbol{s}\mathcal{O}(x_0). \tag{30}$$

In addition, we assume that the integration measure transforms as

$$dX' = dX\left(1 + \int_{\Sigma_h} dx\, \xi(x) \mathcal{A}_s(x)\right). \tag{31}$$

Then, from Eq. (28), we obtain the identity for the vacuum expectation value (vev),

$$\int_{\Sigma_h} dx\, \xi(x) \big\langle \boldsymbol{s}\mathcal{O}(x_0)\delta(x - x_0) - \mathcal{O}(x_0)\,(K_s(x) - \mathcal{A}_s(x))\big\rangle = 0, \tag{32}$$

where the vev is defined by

$$\langle \mathcal{O}(x)\rangle \equiv Z^{-1} \int dX\, \mathcal{O}(x) e^{-S[X]}, \tag{33}$$

with the partition function $Z = \int dX\, e^{-S[X]}$. In particular, if we assume that the parameter $\xi(y)$ takes the form $\xi(y) = \xi\delta(y - x)$ for a specific coordinate x and constant parameter ξ, we obtain the identity for the vev of local variables:

$$\big\langle \mathcal{O}(x_0)\,(K_s(x) - \mathcal{A}_s(x))\big\rangle = \delta(x - x_0)\big\langle \boldsymbol{s}\mathcal{O}(x_0)\big\rangle. \tag{34}$$

[2] We assume that the ranges of the integrations by X and X' are identical.

Let us return to the supersymmetric gauge theory that we are considering. As discussed in the previous subsection, the action of the supersymmetric theory is invariant under the two supersymmetry transformations generated by Q and $\tilde{Q}$, and the two $U(1)$ transformations $U(1)_A$ and $U(1)_V$. Therefore, the transformation of the action in Eq. (2) is given by

$$\delta_s S = \int_{\Sigma_h} dx\, \xi(x) d^\dagger J_s(x)\omega \tag{35}$$

up to total derivative, where $J_s(x)$ is the corresponding Noether current.

Although it is sufficient only to consider the action in Eq. (2) of the continuous theory, we add a further supersymmetry-breaking term to lead to the discussion in the next section:

$$S_\mu = \int_{\Sigma_h} dx\, \mathcal{L}_\mu(x), \tag{36}$$

which is typically assumed to be mass terms. For the total action $S + S_\mu$, $K_s(x)$ is given by

$$K_s(x) = d^\dagger J_s(x)\omega + \boldsymbol{s}\mathcal{L}_\mu(x). \tag{37}$$

Since the integration measure is invariant under the supersymmetry transformations Q and $\tilde{Q}$, the corresponding WT identities are given by

$$\langle \mathcal{O}(x_0) d^\dagger J_Q(x)\omega\rangle = -\langle \mathcal{O}(x_0) Q\mathcal{L}_\mu(x)\rangle + \delta^2(x - x_0)\langle Q\mathcal{O}(x_0)\rangle, \tag{38}$$

$$\langle \mathcal{O}(x_0) d^\dagger J_{\tilde{Q}}(x)\omega\rangle = -\langle \mathcal{O}(x_0) \tilde{Q}\mathcal{L}_\mu(x)\rangle + \delta^2(x - x_0)\langle \tilde{Q}\mathcal{O}(x_0)\rangle. \tag{39}$$

For the $U(1)_A$ symmetry we have to be more careful since the integration measure is *not* invariant under the $U(1)_A$ transformation. Using the so-called Fujikawa's method, we see that

$$dX' = dX \exp\left(i\frac{\dim G}{4\pi}\int_{\Sigma_h}\theta_A(x)R(x)\omega\right), \tag{40}$$

where $R(x)$ is the scalar curvature of Σ_h. This is the case where $\mathcal{A}_s \neq 0$ and is nothing but the $U(1)$ anomaly. Thus, we obtain the WT identity for the $U(1)_A$ symmetries,

$$\left\langle \mathcal{O}(x_0)\left(d^\dagger J_A(x) + \frac{\dim G}{4\pi}R(x)\right)\omega\right\rangle = -\langle \mathcal{O}(x_0)\boldsymbol{s}_A\mathcal{L}_\mu(x)\rangle + \delta^2(x - x_0)\langle \boldsymbol{s}_A\mathcal{O}(x_0)\rangle, \tag{41}$$

where $\boldsymbol{s}_A$ are the generators of the $U(1)_A$ transformation. In particular, by integrating Eq. (41) over Σ_h with $\mathcal{O} = 1$, we obtain

$$\int_{\Sigma_h}\langle d^\dagger J_A\omega\rangle = -\frac{\dim G}{4\pi}\int_{\Sigma_h} R\omega = -\dim G\, \chi_h, \tag{42}$$

where $\chi_h \equiv 2 - 2h$ is the Euler characteristic of Σ_h. Therefore, we see that no anomaly appears on the torus T^2 ($h = 1$).

On the other hand, since the integration measure is invariant under the $U(1)_V$ transformation, the $U(1)_V$ symmetry is not anomalous and the corresponding WT identity symmetry is given by

$$\langle \mathcal{O}(x_0) d^\dagger J_V(x)\omega\rangle = -\langle \mathcal{O}(x_0)\boldsymbol{s}_V\mathcal{L}_\mu(x)\rangle + \delta^2(x - x_0)\langle \boldsymbol{s}_V\mathcal{O}(x_0)\rangle, \tag{43}$$

where $\boldsymbol{s}_V$ is the generator of the $U(1)_V$ transformation.

3. Graph theory for discretized supersymmetric gauge theory

In this section we consider discretization of the Riemann surface in order to regularize the supersymmetric gauge theory discussed in the previous section. Although the discretization method is identical to the model given in Ref. [52], we will reconstruct it from the perspective of graph theory.

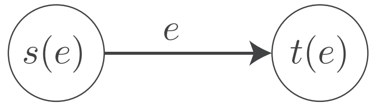

Fig. 1. A piece of the directed graph. $s(e)$ and $t(e)$ represent the "source" and "target" vertices for a given edge e.

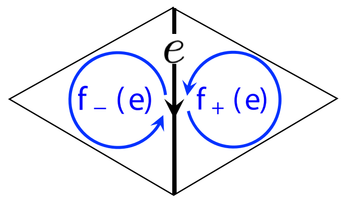

Fig. 2. Another piece of the directed graph. $f_+(e)$ and $f_-(e)$ represent the faces that contain the common edge e in the same direction and the opposite direction for a given edge e.

3.1 *Discretized Riemann surface as a graph*

To regularize the supersymmetric gauge theory considered in the previous section we divide the Riemann surface into polygons, i.e. the continuous Riemann surface is approximated by an object consisting of polyhedra glued together without gaps. We assume that the polyhedra are connected by edges, and that there are no vertices in the middle of the edges. We call each polyhedron that constitutes a polygon a face. As a result, a discretized Riemann surface is labeled by a set of vertices $V = \{v_1, \ldots, v_{n_V}\}$, a set of edges $E = \{e_1, \ldots, e_{n_E}\}$, and a set of faces $F = \{f_1, \ldots, f_{n_F}\}$, where n_V, n_E, and n_F are the numbers of vertices, edges, and faces, respectively. For simplicity, we will consider only Riemann surfaces without boundaries in this paper.

The number of faces that a vertex v shares is equal to the number of edges one of whose ends is v, which we call the degree of the vertex v and denote by $\deg(v)$. Similarly, the number of vertices that a face f shares is equal to the number of edges that consist of f, which we call the degree of the face f and denote by $\deg(f)$. We can assign a direction to every edge. We thus express the edge e starting from vertex v_s and ending at vertex v_t as $e = \{v_s, v_t\}$. We call v_s the source of e and v_t the target of e, and also write $v_s = s(e)$ and $v_t = t(e)$ for given e (see Fig. 1).

Since Riemann surfaces are orientable by definition, we can also consider orientations for the surface f. Here we adopt the right-handed system and define the direction of the face as the counter-clockwise rotation when we see the Riemann surface from the outside. Then, the surface f can be expressed as $f = \{e_{i_1}, \ldots, e_{i_{\deg(f)}}\}$ as a list of its constituent edges along the direction of f. Since we assume no boundary, every edge is shared by two faces, and these two faces contain a common edge in opposite directions by construction. We then write $f_+(e)$ for the face that contains the edge e in the same direction and $f_-(e)$ for the face that contains it in the opposite direction (see Fig. 2).

The observation is that the discretized Riemann surface constructed in this way can be naturally interpreted as a pair of a graph Γ and its dual graph $\check{\Gamma}$. A directed graph is defined as a triple (V, E, φ) where V is a set of vertices, E a set of edges, and φ a map $V \times V \to E$. By considering the relation between V and E constructed above as a map φ: $V \times V \to E$, we can naturally regard the triple (V, E, φ) as a directed graph Γ. Note that in general graphs it is possible to draw two or more edges between two definite vertices, or to draw an edge that returns to the same vertex, but the graph we are considering here has at most one edge between two definite vertices, and does not allow edges connecting the same vertex.

On the other hand, the relationship between the faces and edges constructed above can be regarded as a map $\check{\varphi} : F \times F \to E$, thus $(F, E, \check{\varphi})$ can also be regarded as a graph, which is the dual graph $\check{\Gamma}$ of Γ. Therefore, the polygon partition of the Riemann surface considered above can be regarded as a pair $(\Gamma, \check{\Gamma})$ of a graph and its dual graph.

3.2 *Matrices describing a graph*

We introduce some useful matrices which describe the structures, and examine their properties. These matrices are used not only to define the graph structures, but also to make it possible to use linear algebra to treat the graph. In the following we denote the n_V-, n_E-, and n_F-dimensional vector spaces on V, E, and F as $\mathcal{V}_V$, $\mathcal{V}_E$, and $\mathcal{V}_\mathcal{F}$, respectively. We consider only directed simple graphs.

3.2.1 *Incidence matrix.* The incidence matrix L is a matrix of size $n_E \times n_V$ whose elements are given by

$$L^e{}_v = \begin{cases} +1 & \text{if } t(e) = v, \\ -1 & \text{if } s(e) = v, \\ 0 & \text{otherwise,} \end{cases} \tag{44}$$

which gives a linear mapping $\mathcal{V}_V \to \mathcal{V}_E$ and can be generated uniquely from the mapping φ: $V \times V \to E$ in the triple of the graph. Note that L is essentially the charge matrix of the quiver theory. The matrix L acts on a vector $\boldsymbol{x} = (x^1, \ldots, x^{n_V})^{\mathrm{T}} \in \mathcal{V}_V$ as

$$L\boldsymbol{x} = (x^{t(e_1)} - x^{s(e_1)}, \ldots, x^{t(e_{n_E})} - x^{s(e_{n_E})})^{\mathrm{T}} \in \mathcal{V}_E, \tag{45}$$

which is a generalization of the forward difference in terms of lattice gauge theory. By regarding $\mathcal{V}_V$ and $\mathcal{V}_E$ as analogs of the spaces of 0-forms and 1-forms, L and L^{T} can be seen as analogs of the exterior derivative d and its adjoint $d^\dagger$ in differential geometry.

We see that the equation $L\boldsymbol{x} = 0$ has the unique solution $x^{v_1} = \cdots = x^{v_{n_V}} = c$, since this equation is equivalent to $x^{s(e)} = x^{t(e)}$ and all the vertices are assumed to be connected. Therefore, for a connected graph the rank of the incidence matrix L is $n_V - 1$ and $\ker L = \{c\mathbf{1}_{n_V} \mid c \in \mathbb{C}\}$, where $\mathbf{1}_{n_V} = (1, \ldots, 1)^{\mathrm{T}}$ in general. This is the analog of the fact that the unique solution of $df = 0$ is $f =$ const. in differential geometry. In the following we denote the normalized zero mode of L as

$$\boldsymbol{v}_0 \equiv \frac{1}{\sqrt{n_V}}\mathbf{1}_{n_V}. \tag{46}$$

To specify $\ker L^{\mathrm{T}}$, we consider a closed loop C made of edges with a direction. Correspondingly, we define the vector $\boldsymbol{w}_C \in \mathcal{V}_E$ whose elements are given by

$$(\boldsymbol{w}_C)^e = \begin{cases} 1 & \text{if } C \text{ includes } e \text{ in the same direction,} \\ -1 & \text{if } C \text{ includes } e \text{ in the opposite direction,} \\ 0 & \text{otherwise,} \end{cases} \tag{47}$$

which we call the loop vector associated with the loop C. The loop vector $\boldsymbol{w}_C$ satisfies $L^{\mathrm{T}}\boldsymbol{w}_C = 0$ since, for a fixed vertex v in the loop C, there are two edges e_1 and e_2 in C which have an end on v, and the values of the products ${L^{\mathrm{T}}}^v{}_{e_1}(\boldsymbol{w}_C)^{e_1}$ and ${L^{\mathrm{T}}}^v{}_{e_2}(\boldsymbol{w}_C)^{e_2}$ are always opposite and cancel with each other by construction. Therefore, all the loop vectors $\boldsymbol{w}_C$ are elements of $\ker L^{\mathrm{T}}$.

Furthermore, by counting the dimension we see that $\ker L^{\mathrm{T}}$ is generated by linearly independent loop vectors. First of all, we can construct n_F loop vectors $\boldsymbol{w}_f$ associated with each face $f \in F$. They are not linearly independent but have one dependence, $\sum_{f\in F} \boldsymbol{w}_f = 0$, so we can construct $n_F - 1$ linearly independent loop vectors. In addition, there are $2h$ independent non-contractible cycles on the genus-h Riemann surface. Since the loop vectors $\boldsymbol{w}_I$ ($I = 1, \ldots, 2h$) corresponding to the cycles cannot be constructed from $\boldsymbol{w}_f$, the $n_F + 2h - 1$ vectors $\{\boldsymbol{w}_f, \boldsymbol{w}_I\}$ are linearly independent. Recalling here that the rank of L is $n_V - 1$, we find $\dim \ker L^{\mathrm{T}} = n_E - n_V + 1 = n_F + 2h - 1$. Therefore, we can conclude that $\{\boldsymbol{w}_f, \boldsymbol{w}_I\}$ could form a basis of $\ker L^{\mathrm{T}}$.

For later use, we also introduce a matrix (unoriented incidence matrix) of size $n_E \times n_V$:

$$K^e_{\ v} \equiv |L^e_{\ v}| = \begin{cases} 1 & \text{if } t(e) = v \text{ or } s(e) = v, \\ 0 & \text{otherwise.} \end{cases} \tag{48}$$

3.2.2 *Dual incidence matrix.* We can also define the incidence matrix $\check{L}$ for the dual graph $\check{\Gamma}$, which is a matrix of size $n_E \times n_F$ whose elements are given by

$$\check{L}^e_{\ f} = \begin{cases} +1 & \text{if the edge } e \text{ on the face } f \text{ is in the forward direction,} \\ -1 & \text{if the edge } e \text{ on the face } f \text{ is in the reverse direction,} \\ 0 & \text{otherwise.} \end{cases} \tag{49}$$

We call this matrix the dual incidence matrix. As well as the incidence matrix, if we restrict ourselves to the relationship between E and F, $\check{L}$ and $\check{L}^{\mathrm{T}}$ correspond to $d^\dagger$ and d in the differential geometry. By repeating the same discussion as for L, we see that $\ker \check{L}$ is the one-dimensional vector space generated by the constant vector, $\ker \check{L} = \{c\mathbf{1}_{n_F} \mid c \in \mathbb{C}\}$, and $\ker \check{L}^{\mathrm{T}}$ is generated by independent dual loop vectors whose dimension is $n_V + 2h - 1$. We denote the normalized zero mode of $\check{L}$ by

$$\boldsymbol{u}_0 \equiv \frac{1}{\sqrt{n_F}} \mathbf{1}_{n_F}, \tag{50}$$

as in the case of the incidence matrix.

We also introduce the unoriented dual incidence matrix by

$$\check{K}^e_{\ f} \equiv |\check{L}^e_{\ f}| = \begin{cases} 1 & \text{if the face } f \text{ includes the edge } e, \\ 0 & \text{otherwise.} \end{cases} \tag{51}$$

3.2.3 *Laplacian matrices.* The Laplacian (Kirchhoff) matrix Δ_V acting on the vertex is an $n_V \times n_V$ matrix defined by

$$(\Delta_V)^v_{\ v'} = L^{\mathrm{T}} L = \begin{cases} \deg(v) & \text{if } v = v', \\ -1 & \text{if } v \neq v' \text{ and } v \text{ is adjacent to } v', \\ 0 & \text{otherwise,} \end{cases} \tag{52}$$

which is also known as the Cartan matrix on the Dynkin diagram (graph) for the Lie algebra. Note that this matrix is called "Laplacian" since it acts on $\boldsymbol{x}$ like

$$\boldsymbol{x}^{\mathrm{T}} \Delta_V \boldsymbol{x} = \sum_{e\in E} (x^{t(e)} - x^{s(e)})^2, \tag{53}$$

which is nothing but a second-order difference operator for the "field" x^v. This also supports the analogy $L \leftrightarrow d$ and $L^{\mathrm{T}} \leftrightarrow d^\dagger$ because the Laplacian acting on a 0-form f is $\Delta f = d^\dagger df$ in differential geometry.

We also define the face Laplacian matrix Δ_F by

$$(\Delta_F)^f{}_{f'} = \check{L}^{\mathrm{T}}\check{L} = \begin{cases} \deg(f) & \text{if } f = f', \\ -1 & \text{if } f \text{ and } f' \text{ share the same edge}, \\ 0 & \text{otherwise}, \end{cases} \tag{54}$$

and the edge Laplacian by

$$\Delta_E \equiv LL^{\mathrm{T}} + \check{L}\check{L}^{\mathrm{T}}. \tag{55}$$

3.2.4 *Cohomology of L and Ľ and the eigenvalues of the Laplacian matrices.* The incidence and dual incidence matrices represent maps from $\mathcal{V}_V$ to $\mathcal{V}_E$ and from $\mathcal{V}_F$ to $\mathcal{V}_E$, respectively. Furthermore, the incidence and dual incidence matrices are orthogonal to each other,

$$L^{\mathrm{T}}\check{L} = \check{L}^{\mathrm{T}}L = 0, \tag{56}$$

which holds for the same reason that the loop vectors belong to the kernel of L^{T}. This is an analog of the nilpotency (exactness) of the differential d and $d^{\dagger}$. This means that we can construct the following exact sequences:

$$\begin{aligned} &0 \to \mathcal{V}_V \xrightarrow{L} \mathcal{V}_E \xrightarrow{\check{L}^{\mathrm{T}}} \mathcal{V}_F \to 0, \\ &0 \leftarrow \mathcal{V}_V \xleftarrow{L^{\mathrm{T}}} \mathcal{V}_E \xleftarrow{\check{L}} \mathcal{V}_F \leftarrow 0. \end{aligned} \tag{57}$$

Because of this nilpotency, we can define the cohomology group $H^V = \ker L$, $H^E = \ker \check{L}^{\mathrm{T}} / \operatorname{im} L$, and $H^F = \mathcal{V}_F / \operatorname{im} \check{L}^{\mathrm{T}}$.

Similar to Hodge's theorem on a compact orientable Riemannian manifold, the cohomology group is isomorphic to a set of the kernel of the Laplacian (harmonic forms). As mentioned in the previous subsection, $\dim\ker L = \dim\ker \check{L} = 1$ and thus we see that

$$\dim\ker \Delta_V = \dim H^V = 1, \tag{58}$$

$$\dim\ker \Delta_F = \dim H^F = 1. \tag{59}$$

More explicitly, $\ker \Delta_V$ and $\ker \Delta_F$ are generated by $\boldsymbol{v}_0$ and $\boldsymbol{u}_0$, respectively. Similarly, since $\dim\ker \check{L}^{\mathrm{T}} = n_V + 2h - 1$ and $\dim \operatorname{im} L = n_V - 1$, we see that

$$\dim\ker \Delta_E = \dim H^E = 2h. \tag{60}$$

Note that these results are consistent with the definition of the Euler characteristic of the graph Γ,

$$\chi_h = \dim H^V - \dim H^E + \dim H^F = 2 - 2h. \tag{61}$$

In the following argument, the eigenvectors of the Laplacian matrices play important roles. Since $\operatorname{rank} L = n_V - 1$ and $\operatorname{rank} \check{L} = n_F - 1$, the ranks of Δ_V and Δ_F are $n_V - 1$ and $n_F - 1$, respectively. Therefore, in addition to the normalized zero modes $\boldsymbol{v}_0$ and $\boldsymbol{u}_0$ given by Eqs. (46) and (50), Δ_V and Δ_F have respectively $n_V - 1$ and $n_F - 1$ linearly independent eigenvectors with non-zero eigenvalues. We then denote the orthonormal eigenvectors of Δ_V and Δ_F as $\{\boldsymbol{v}_0, \boldsymbol{v}_i\}$ ($i = 1, \ldots, n_V - 1$) and $\{\boldsymbol{u}_0, \boldsymbol{u}_a\}$ ($a = 1, \ldots, n_F - 1$), with

$$\begin{aligned} &\Delta_V \boldsymbol{v}_0 = 0, \quad \Delta_V \boldsymbol{v}_i = \lambda_i \boldsymbol{v}_i \quad (\lambda_i \neq 0), \\ &\Delta_F \boldsymbol{u}_0 = 0, \quad \Delta_F \boldsymbol{u}_a = \mu_a \boldsymbol{u}_a \quad (\mu_a \neq 0), \end{aligned} \tag{62}$$

respectively.

$L\boldsymbol{v}_i$ and $\check{L}\boldsymbol{u}_a$ become simultaneously eigenvectors of Δ_E with eigenvalues λ_i and μ_a, respectively, since

$$\begin{aligned}\Delta_E(L\boldsymbol{v}_i) &= L\Delta_V\boldsymbol{v}_i = \lambda_i(L\boldsymbol{v}_i),\\ \Delta_E(\check{L}\boldsymbol{u}_a) &= \check{L}\Delta_F\boldsymbol{u}_a = \mu_a(\check{L}\boldsymbol{u}_a),\end{aligned} \tag{63}$$

where we have used the relation in Eq. (56). We then normalize them by

$$\boldsymbol{e}_i \equiv L\boldsymbol{v}_i/|L\boldsymbol{v}_i|, \qquad \boldsymbol{e}_a \equiv \check{L}\boldsymbol{u}_a/|\check{L}\boldsymbol{u}_a|, \tag{64}$$

which are orthogonal vectors in $\mathcal{V}_E$. To complete the orthonormal basis of $\mathcal{V}_E$, we need to add $2h$ independent normalized vectors $\{\boldsymbol{e}_0^I\}$ ($I = 1, \ldots, 2h$), which belong to $\ker\Delta_E$, since $\dim\mathcal{V}_E = n_E = (n_V - 1) + (n_F - 1) + 2h$ and $\dim\ker\Delta_E = 2h$. Therefore, the orthonormal eigenvectors of Δ_E are spanned by $\{\boldsymbol{e}_0^I, \boldsymbol{e}_i, \boldsymbol{e}_a\}$, which satisfy

$$\Delta_E\boldsymbol{e}_0^I = 0, \qquad \Delta_E\boldsymbol{e}_i = \lambda_i\boldsymbol{e}_i, \qquad \Delta_E\boldsymbol{e}_a = \mu_a\boldsymbol{e}_a. \tag{65}$$

From the argument below Eq. (47), we find that the zero eigenvectors $\boldsymbol{e}_0^I$ correspond to the independent non-contractible cycles on the graph Γ. Note also that the non-zero eigenvalues of Δ_E are common with those of Δ_V and Δ_F, namely

$$\mathrm{Spec}'\,\Delta_V \oplus \mathrm{Spec}'\,\Delta_F = \mathrm{Spec}'\,\Delta_E, \tag{66}$$

where Spec$'$ stands for a set of non-zero eigenvalues (spectrum) of the Laplacian.

4. Abelian gauge theory on the graph

In this section we formulate a supersymmetric Abelian gauge theory on the discretized Riemann surface by using graph theory. We will see that restricting the theory to Abelian makes it easier to see the zero mode structure of the theory, but will also give us important insights into the relationship between anomalies and zero modes.

4.1 *Definition of the model*

We define several vectors on the vertices, edges, and faces, which are regarded as fields. To define a covariant theory using these fields, we have to consider a metric structure. To this end, we introduce contravariant and covariant vectors, which are expressed as vectors with upper and lower indices, respectively.

We consider an n_V-dimensional bosonic vector $\boldsymbol{\phi} = (\phi^1, \phi^2, \ldots, \phi^{n_V})^{\mathrm{T}}$ and the complex conjugate $\bar{\boldsymbol{\phi}} = (\bar{\phi}^1, \bar{\phi}^2, \ldots, \bar{\phi}^{n_V})^{\mathrm{T}}$, whose elements ϕ^v and $\bar{\phi}^v$ are regarded as complex bosonic variables (fields) living on the vertex $v \in V$. Note that the positioning of the indices is important: the elements of $\boldsymbol{\phi}$ and $\bar{\boldsymbol{\phi}}$ have upper indices that indicate they are contravariant vectors. If we take the transpose, they become covariant vectors, which have lower indices: $\boldsymbol{\phi}^{\mathrm{T}} = (\phi_1, \phi_2, \ldots, \phi_{n_V})$ and $\bar{\boldsymbol{\phi}}^{\mathrm{T}} = (\bar{\phi}_1, \bar{\phi}_2, \ldots, \bar{\phi}_{n_V})$.

We also consider an n_E-dimensional bosonic vector $\boldsymbol{U} = (U^1, U^2, \ldots, U^{n_E})^{\mathrm{T}}$, which will be gauge fields, whose elements are assumed to take the values in $U(1)$. In this case, we can write $\boldsymbol{U}$ by $\exp\{i\boldsymbol{A}\}$, where $\boldsymbol{A} = (A^1, A^2, \ldots, A^{n_E})^{\mathrm{T}}$, whose elements are real variables. Furthermore, we introduce an n_F-dimensional bosonic vector $\boldsymbol{Y} = (Y^1, Y^2, \ldots, Y^{n_F})^{\mathrm{T}}$ whose elements are assumed to be real. In addition to the bosonic fields, we also consider the fermionic fields $\boldsymbol{\eta} = (\eta^1, \eta^2, \ldots, \eta^{n_V})^{\mathrm{T}} \in \mathcal{V}_V$, $\boldsymbol{\lambda} = (\lambda^1, \lambda^2, \ldots, \lambda^{n_E})^{\mathrm{T}} \in \mathcal{V}_E$, and $\boldsymbol{\chi} = (\chi^1, \chi^2, \ldots, \chi^{n_F})^{\mathrm{T}} \in \mathcal{V}_F$.

We define the supersymmetry transformations of these fields by

$$\begin{aligned}
&Q\phi^v = 0, && \\
&Q\bar{\phi}^v = 2\eta^v, && Q\eta^v = 0, \\
&QA^e = \lambda^e, && Q\lambda^e = -L^e{}_v\phi^v, \\
&QY^f = 0, && Q\chi^f = Y^f.
\end{aligned} \tag{67}$$

Using this symmetry, we write the action of the model in the Q-exact form as

$$S = -\frac{1}{2g^2} Q\left\{\bar{\phi}_v L^{\mathrm{T}v}{}_e\lambda^e + \chi_f(Y^f - 2\mu(P^f))\right\}, \tag{68}$$

where P^f are the plaquette variables associated with the face f, defined by

$$P^f \equiv \prod_{e\in f}(U^e)^{\check{L}^{\mathrm{T}f}{}_e} = \exp\left\{i\check{L}^{\mathrm{T}f}{}_e A^e\right\}, \tag{69}$$

and $\mu(P^f)$ is a function called the moment map, which becomes the field strength F in the continuum limit.

There are several candidates for the moment map. The moment map used in the original Sugino model is

$$\mu(P) = \frac{1}{2i}\frac{P - P^\dagger}{1 - \frac{1}{\epsilon^2}||1 - P||^2}, \tag{70}$$

where $||\cdot||$ is a matrix norm defined by $||A|| \equiv \sqrt{\mathrm{tr}(AA^\dagger)}$, which is now simply $||A|| = |A|^2$ in the Abelian theory, and ϵ is a positive constant parameter chosen in the range $0 < \epsilon < 2$. If we do not introduce the denominator, the vacuum condition $\mu(P) = 0$ has two solutions $P = \pm 1$ which contain an unphysical vacuum at $P = -1$. The denominator is necessary to avoid it. See Ref. [5] for more detail.

Another candidate is the tangent-type function

$$\mu(P) = \frac{1}{2i}\frac{P - P^\dagger}{P + P^\dagger} \tag{71}$$

proposed in Ref. [50]. $P = -1$ is on the pole of this function and thus $\mu(P) = 0$ has a unique solution at the physical vacuum.

In addition, in Abelian theory we can use a logarithmic-type moment map,

$$\mu(P) = -i\log(P). \tag{72}$$

Although this suffers from the mathematical difficulty of defining the log of a matrix in non-Abelian theory, there is no ambiguity in Abelian theory by choosing the branch of the logarithmic function as $-\pi < \arg z \leq \pi$ for $z \in \mathbb{C}$.

After eliminating the auxiliary field Y^f, the bosonic part of the action becomes

$$S_{\mathrm{B}} = \frac{1}{2g^2}\left\{\bar{\phi}_v L^{\mathrm{T}v}{}_e L^e{}_{v'}\phi^{v'} + \mu(P^f)^2\right\} = \frac{1}{2g^2}\left\{\bar{\boldsymbol{\phi}}^{\mathrm{T}}\Delta_V\boldsymbol{\phi} + |\boldsymbol{\mu}|^2\right\}, \tag{73}$$

where we have used the definition of the graph vertex Laplacian $\Delta_V = L^{\mathrm{T}}L$ and defined $\boldsymbol{\mu} \equiv (\mu(P^{f_1}), \ldots, \mu(P^{f_{n_F}}))^{\mathrm{T}}$. This action describes the free complex scalar field decoupling from Maxwell theory in the continuum limit.

The fermionic part of the action becomes

$$S_{\mathrm{F}} = -\frac{1}{g^2}\left\{\eta_v L^{\mathrm{T}v}{}_e\lambda^e + \chi_f\frac{\delta\mu^f}{\delta A^e}\lambda^e\right\} = -\frac{1}{g^2}\left\{\boldsymbol{\eta}^{\mathrm{T}}L^{\mathrm{T}}\boldsymbol{\lambda} + \boldsymbol{\chi}^{\mathrm{T}}\frac{\delta\boldsymbol{\mu}}{\delta\boldsymbol{A}}\boldsymbol{\lambda}\right\}, \tag{74}$$

where $\frac{\delta \boldsymbol{\mu}}{\delta \boldsymbol{A}}$ is an $n_F \times n_E$ matrix and is proportional to the transpose of the dual incidence matrix $\check{L}^{\mathrm{T}}$. Indeed, for each component, we find

$$\frac{\delta \mu(P^f)}{\delta A^e} = i\mu'(P^f)P^f \check{L}^{\mathrm{T}f}{}_e, \tag{75}$$

where μ' stands for a derivative of the function μ with respect to the argument.

This model is nothing but the Abelian version of the generalized Sugino model constructed in Ref. [52]. Repeating the discussion in Ref. [52], we see that this model is a discretization of the $\mathcal{N} = (2, 2)$ supersymmetric Abelian gauge theory discussed in Sect. 2. Because of the discretization, the $\tilde{Q}$ symmetry and the $U(1)_V$ symmetries are explicitly broken, while the Q symmetry and the $U(1)_A$ symmetry are still preserved after discretization, at least classically.

4.2 *Fermion zero modes*

Here we will examine the structure of the fermions in this theory. We first redefine χ^f by

$$\rho^f \equiv i\mu'(P^f)P^f \chi^f, \tag{76}$$

where we assume that the prefactor $i\mu'(P^f)P^f$ is non-vanishing and non-singular everywhere.[3] Then we combine all the fermionic variables into a single $(n_V + n_F + n_E)$-dimensional vector such that

$$\boldsymbol{\Psi} = \begin{pmatrix} \boldsymbol{\eta} \\ \boldsymbol{\rho} \\ \boldsymbol{\lambda} \end{pmatrix}. \tag{77}$$

Then, the fermionic part of the action in Eq. (74) can be written as

$$S_{\mathrm{F}} = \frac{1}{g^2} \boldsymbol{\Psi}^{\mathrm{T}} i \not{D} \boldsymbol{\Psi}, \tag{78}$$

where $\not{D}$ is a matrix of size $(n_V + n_F + n_E)$,

$$\not{D} = \begin{pmatrix} 0 & iD^{\mathrm{T}} \\ -iD & 0 \end{pmatrix}, \tag{79}$$

with

$$D = \begin{pmatrix} L & \check{L} \end{pmatrix}. \tag{80}$$

We examine the zero modes of the matrix $\not{D}$, which can be obtained from the zero modes of D and D^{T}.

D is a linear mapping from $\mathcal{V}_V \oplus \mathcal{V}_F$ to $\mathcal{V}_E$ which transforms $(\boldsymbol{\eta}, \boldsymbol{\rho})^{\mathrm{T}} \in \mathcal{V}_V \oplus \mathcal{V}_F$ as

$$D \begin{pmatrix} \boldsymbol{\eta} \\ \boldsymbol{\rho} \end{pmatrix} = L\boldsymbol{\eta} + \check{L}\boldsymbol{\rho}. \tag{81}$$

Recalling that $\dim \ker L = \dim \ker \check{L} = 1$, we can immediately see that D has one zero mode in $\boldsymbol{\eta}$ and $\boldsymbol{\rho}$, each[4] proportional to $\boldsymbol{v}_0$, Eq. (46), and $\boldsymbol{u}_0$, Eq. (50), respectively. Therefore, we find that rank $D = n_V + n_F - 2 = n_E - 2h$, where we have used the definition $\chi_h = n_V - n_E + n_F = 2 - 2h$.

[3]The argument in this subsection always holds for χ^f itself in the saddle point approximation, where $\rho^f \sim i\chi^f$ with $P^f \sim 1$. In the localization method, the zero modes of χ^f play the same role as the zero modes of ρ^f.

[4]Note that the equation $L\boldsymbol{\eta} + \check{L}\boldsymbol{\rho} = 0$ leads to $L\boldsymbol{\eta} = \check{L}\boldsymbol{\rho} = 0$ because of the orthogonality in Eq. (56).

On the other hand, D^{T} is a linear mapping from $\mathcal{V}_E$ to $\mathcal{V}_V \oplus \mathcal{V}_F$ which transforms $\boldsymbol{\lambda} \in \mathcal{V}_E$ as

$$D^{\mathrm{T}}\boldsymbol{\lambda} = \begin{pmatrix} L^{\mathrm{T}}\boldsymbol{\lambda} \\ \check{L}^{\mathrm{T}}\boldsymbol{\lambda} \end{pmatrix}. \tag{82}$$

Then, the zero modes of D^{T} are the common zero modes of L^{T} and $\check{L}^{\mathrm{T}}$, which are the same as the zero modes $\{\boldsymbol{e}_0^I\}$ of Δ_E. This is a direct result of the isomorphism $\ker LT/\operatorname{im}\check{L} \simeq \ker \Delta_E$, i.e. $\ker L^{\mathrm{T}}$ is spanned by the $n_F + 2h - 1$ linearly independent loop vectors $\{\boldsymbol{e}_0^I, \boldsymbol{w}_a\}$, where $\boldsymbol{w}_a$ ($a = 1, \ldots, n_F - 1$) are linearly independent loop vectors corresponding to the faces, and $\operatorname{im}\check{L}$ is spanned by $\{\boldsymbol{w}_a\}$ by construction. Therefore, $\ker \Delta_E$ is spanned by $\{\boldsymbol{e}_0^I\}$.

In summary, $\not{D}$ has one zero mode η_0 in $\boldsymbol{\eta}$, one zero mode ρ_0 in $\boldsymbol{\rho}$, and $2h$ zero modes λ_0^I ($I = 1, \ldots, 2h$) in $\boldsymbol{\lambda}$, which can be written explicitly as

$$\eta_0 = \boldsymbol{v}_0 \cdot \boldsymbol{\eta}, \qquad \rho_0 = \boldsymbol{u}_0 \cdot \boldsymbol{\rho}, \qquad \lambda_0^I = \boldsymbol{e}_0^I \cdot \boldsymbol{\lambda}. \tag{83}$$

Note that the vertex zero mode η_0 and the edge zero modes λ_0^I are Q-invariant, while the face zero mode ρ_0 is not. The Q-invariance of η_0 is trivial from Eq. (67), and λ_0^I is Q-invariant since the loop vector $\boldsymbol{e}_0^I$ belongs to $\ker L^{\mathrm{T}}$. However, Q transforms χ_0' as

$$\begin{aligned} Q\rho_0 &= \frac{1}{\sqrt{n_F}} \sum_{f\in F} Q(i\mu'(P^f)P^f\chi^f) \\ &= \frac{1}{\sqrt{n_F}} \sum_{f\in F} \left\{ -\left(\mu''(P^f)(P^f)^2 + \mu'(P^f)P^f\right)\lambda^e \check{L}^e{}_f \chi^f + i\mu'(P^f)P^f Y^f \right\}, \end{aligned} \tag{84}$$

which does not vanish in general.

4.3 *Heat kernel and dimensionality*

We can examine the analytic behavior of the fermion spectrum by using the heat kernel. In the continuous theory, the heat kernel is defined by the following heat equation:

$$\left(\frac{\partial}{\partial t} + \not{D}^2\right) h(x, y; t) = 0, \tag{85}$$

which is formally solved as

$$h(x, y; t) = e^{-t\not{D}^2}. \tag{86}$$

In particular, the regularized $U(1)_A$ current is evaluated by the heat kernel:

$$\int_{\Sigma_h} \left\langle d^\dagger J_A \omega \right\rangle_{\mathrm{reg}} = -\operatorname{Tr}\gamma_A e^{-t\not{D}^2} = -\operatorname{ind}\not{D}. \tag{87}$$

We can extend the definition of the heat kernel to the Dirac operator on the graph. The heat kernel on the graph is simply defined by

$$h(t)^i{}_j \equiv \left(e^{-t\not{D}^2}\right)^i{}_j \tag{88}$$

using the matrix $\not{D}$ defined by Eq. (79). Correspondingly, we define the quantity

$$\begin{aligned} I(t) &\equiv \operatorname{Tr}_{V\oplus F\oplus E}\gamma_A e^{-t\not{D}^2} \\ &= \operatorname{Tr}_V e^{-t\Delta_V} + \operatorname{Tr}_F e^{-t\Delta_F} - \operatorname{Tr}_E e^{-t\Delta_E} \\ &= \sum_{l=1}^{n_V} e^{-t\lambda_l^V} + \sum_{m=1}^{n_F} e^{-t\lambda_m^F} - \sum_{n=1}^{n_E} e^{-t\lambda_n^E}, \end{aligned} \tag{89}$$

where λ_l^V, λ_m^F, and λ_n^E are eigenvalues for the Laplacians Δ_V, Δ_F, and Δ_E, respectively.

In the large-t limit, the contribution of the non-zero modes (eigenvalues) to $I(t)$ disappears and the difference in the number of zero modes survives as the index. Moreover, the contributions from the non-zero modes cancel each other even when the value of t is finite because there is a one-to-one correspondence between the non-zero modes of $\{\Delta_V, \Delta_F\}$ and Δ_E as shown in Sect. 3.2.4. Therefore, $I(t)$ is independent of t, i.e. $I(t)$ gives the index of $\not{D}$ which is equal to the Euler characteristic of the graph, as well as in the continuous theory.

It is instructive to give some concrete examples of the trace of heat kernels. The simplest example of a graph with genus zero is the tetrahedron ($(n_V, n_F, n_E) = (4, 4, 6)$). The eigenvalues of the Laplacians are given by

$$\begin{aligned} \operatorname{Spec} \Delta_V &= \{4, 4, 4, 0\}, \\ \operatorname{Spec} \Delta_F &= \{4, 4, 4, 0\}, \\ \operatorname{Spec} \Delta_E &= \{4, 4, 4, 4, 4, 4\}. \end{aligned} \tag{90}$$

Then, we get

$$\operatorname{Tr} \gamma_A e^{-t\not{D}^2} = (3e^{-4t} + 1) + (3e^{-4t} + 1) - 6e^{-4t} = 2, \tag{91}$$

where the non-zero modes cancel each other order by order.

Similarly, for the hexahedron ($(n_V, n_F, n_E) = (8, 6, 12)$) we obtain

$$\begin{aligned} \operatorname{Spec} \Delta_V &= \{6, 4, 4, 4, 2, 2, 2, 0\}, \\ \operatorname{Spec} \Delta_F &= \{6, 6, 4, 4, 4, 0\}, \\ \operatorname{Spec} \Delta_E &= \{6, 6, 6, 4, 4, 4, 4, 4, 4, 2, 2, 2\}, \end{aligned} \tag{92}$$

and we get

$$\begin{aligned} \operatorname{Tr} \gamma_A e^{-t\not{D}^2} = &(e^{-6t} + 3e^{-4t} + 3e^{-2t} + 1) + (2e^{-6t} + 3e^{-4t} + 1) \\ &- (3e^{-6t} + 6e^{-4t} + 3e^{-2t}) = 2. \end{aligned} \tag{93}$$

For genus 1, the spectrum of the Laplacians of the 3×3 torus are

$$\begin{aligned} \operatorname{Spec} \Delta_V &= \{6, 6, 6, 6, 3, 3, 3, 3, 0\}, \\ \operatorname{Spec} \Delta_F &= \{6, 6, 6, 6, 3, 3, 3, 3, 0\}, \\ \operatorname{Spec} \Delta_E &= \{6, 6, 6, 6, 6, 6, 6, 6, 3, 3, 3, 3, 3, 3, 3, 3, 0, 0\}, \end{aligned} \tag{94}$$

and the index becomes

$$\operatorname{Tr} \gamma_A e^{-t\not{D}^2} = (4e^{-6t} + 4e^{-3t} + 1) + (4e^{-6t} + 4e^{-3t} + 1) - (8e^{-6t} + 8e^{-3t} + 2) = 0, \tag{95}$$

as expected.

Furthermore, the behavior of the heat kernel for each Laplacian (not the square of the Dirac operator) also represents the dimensionality of the graph structure. If we take the continuum limit of the graph discretization (lattice), we expect that the space-time goes to the smooth Riemann surface. The heat kernel on the Riemann surface, which satisfies the heat equation

$$\left(\frac{\partial}{\partial t} + \Delta_x \right) h(x, y; t) = 0 \tag{96}$$

with the Laplacian Δ_x, behaves as

$$h(x, y; t) = \frac{1}{4\pi t} e^{-|x-y|/2t} + \cdots \tag{97}$$

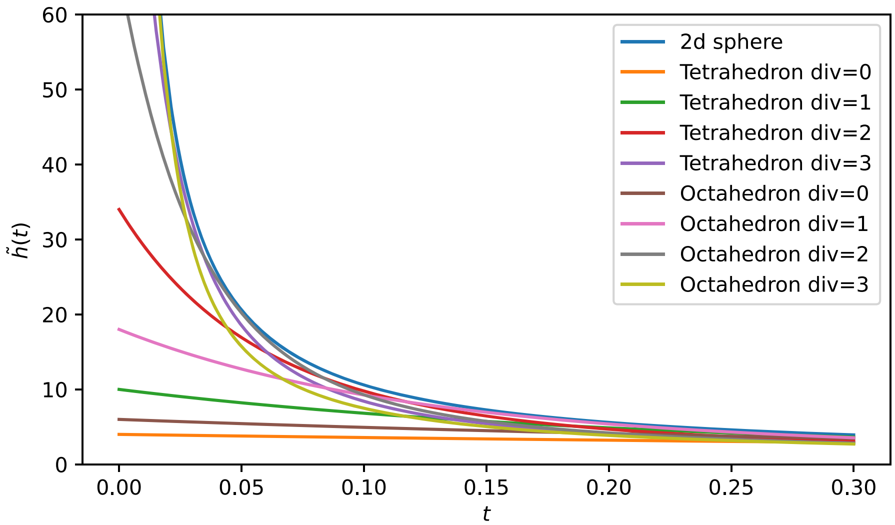

Fig. 3. Plots of the heat kernel. If the number of vertices (or faces) of the geodesic polyhedra is large, the behavior of the heat kernel becomes very close to that of the smooth two-dimensional sphere. (The "div" in the legend stands for the number of times the triangular faces of the tetrahedron or octahedron are divided into smaller triangles.).

for small t, while the index in Eq. (87) is independent of t. In particular, the trace of the heat kernel behaves as

$$\tilde{h}(t) \equiv \int_{\Sigma_h} dx\, h(x, x; t) = \frac{\mathrm{Vol}(\Sigma_h)}{4\pi t} + \cdots , \tag{98}$$

and, in the large-t limit, the trace of the heat kernel tends to the number of zero modes,

$$\lim_{t\to\infty} \tilde{h}(t) = \lim_{t\to\infty} \sum_n e^{-t\lambda_n} = \dim \ker \Delta_V . \tag{99}$$

On the general D-dimensional space-time, the trace of the heat kernel is proportional to $1/t^{D/2}$ for small t. So, if we investigate the small-t behavior of the heat kernel for the graph Laplacian, we can confirm how the dimensionality of the graph discretization is close to the Riemann surface.

We construct the heat kernels of the graph Laplacian for several geodesic polyhedrons with genus 0 (subdivisions of the tetrahedron and octahedron) and plot them in Fig. 3. We find that the behavior of the heat kernel approaches that of the two-dimensional sphere ($1/t$ behavior) as the number of vertices increases and the discretization becomes finer. We also find that the trace of the heat kernel represents the number of zero modes in the large-t limit.

4.4 *Uplifting the fermion zero modes*

Due to the existence of these zero modes, the discretized theory with the action in Eq. (68) is not well-defined since the partition function trivially vanishes. we expand the fermion fields by the eigenvectors of the Laplacian matrices as

$$\boldsymbol{\eta} = \eta_0 \boldsymbol{v}_0 + \sum_{i=1}^{n_V-1} \eta_i \boldsymbol{v}_i,$$

$$\boldsymbol{\chi} = \chi_0 \boldsymbol{u}_0 + \sum_{a=1}^{n_F-1} \chi_a \boldsymbol{u}_a,$$

$$\boldsymbol{\lambda} = \sum_{I=1}^{2h} \lambda_0^I \boldsymbol{e}_0^I + \sum_{i=1}^{n_V-1} \lambda_i \boldsymbol{e}_i + \sum_{a=1}^{n_F-1} \lambda_a \boldsymbol{e}_a \tag{100}$$

and write the integration measure for the modes as $d\mathcal{B}d\mathcal{F}d\mathcal{F}_0$, where

$$d\mathcal{B} = \left(\prod_{v=1}^{n_V} d\phi_v d\bar{\phi}_v\right)\left(\prod_{e=1}^{n_E} dU_e\right), \tag{101}$$

$$d\mathcal{F} = \left(\prod_{i=1}^{n_V-1} d\eta_i d\lambda_i\right)\left(\prod_{a=1}^{n_F-1} d\chi_a d\lambda_a\right), \tag{102}$$

$$d\mathcal{F}_0 = \left(\prod_{I=1}^{2h} d\lambda_0^{2h-I+1}\right) d\chi_0 d\eta_0. \tag{103}$$

Evaluating the vev of a (not necessarily local) operator $\mathcal{O}[X]$, which is a functional of the collective expression of all the fields X and does not include any fermion zero mode, the integration $\int d\mathcal{B}d\mathcal{F}d\mathcal{F}_0\, \mathcal{O}[X]e^{-S[X]}$ trivially vanishes.

To avoid this, we need to insert all the fermion zero modes in the background, like

$$\mathcal{I}_{\mathcal{O}} \equiv \int d\mathcal{B}d\mathcal{F}d\mathcal{F}_0 \left(\eta_0 \chi_0 \prod_{I=1}^{2h} \lambda_0^I\right) \mathcal{O}[X]e^{-S[X]}. \tag{104}$$

The inserted zero modes are integrated by the measure $d\mathcal{F}_0$, and then

$$\mathcal{I}_{\mathcal{O}} = \int d\mathcal{B}d\mathcal{F}\, \mathcal{O}[X]e^{-S[X]} \tag{105}$$

becomes well-defined since the measure no longer includes the fermion zero modes.

The straightforward way to achieve this automatically is to add mass terms of the fermion zero modes to the action as

$$S_\mu = \frac{\mu_0}{g^2}(\eta_0\chi_0) + \frac{\mu_1}{g^2}\sum_{k=1}^{h} \lambda_0^{2k-1}\lambda_0^{2k} \equiv \frac{1}{2g^2}\boldsymbol{\Psi}^{\mathrm{T}}\mathcal{M}\boldsymbol{\Psi}. \tag{106}$$

These terms not only make the Dirac matrix invertible but also supply the necessary fermion zero modes in evaluating correlation functions as

$$\int d\mathcal{B}d\mathcal{F}d\mathcal{F}_0\, \mathcal{O}[X]e^{-S[X]-S_\mu} = \frac{\mu_0\mu_1^h}{g^{2h+2}}\mathcal{I}_{\mathcal{O}}. \tag{107}$$

The necessary fermion zero modes are supplied by expanding e^{-S_μ} by the parameters μ_0 and μ_1 as the term with the coefficient $\mu_0\mu_1^h$, and the other terms vanish as a lack or excess of fermion zero modes. Note that the situation is the same when the operator $\mathcal{O}$ includes all or some of the fermion zero modes, where only the term including all the fermion zero modes survives.

Here we note that the zero modes supplied from e^{-S_μ} break the $U(1)_A$ symmetry unless $h = 1$, reflecting the quantum anomaly discussed below. We also note that the mass terms in Eq. (106) also break the Q symmetry softly since χ_0 is not Q-invariant, as shown in Eq. (84). As discussed in the next section, it is possible to construct such mass terms that cancel the fermion zero modes while preserving the Q symmetry. In this sense, although the mass term constructed here is simple, it is not the only option. In particular, when discussing situations where supersymmetry plays an important role, we should use the Q-invariant mass terms. However, the choice of mass term is not so important in discussing the anomalous $U(1)_A$ current, as long as the partition function is well-defined. Therefore, in this section we will use the regularized action

$$S = \frac{1}{2g^2}\left\{\bar{\boldsymbol{\phi}}^{\mathrm{T}}\Delta_V\boldsymbol{\phi} + |\boldsymbol{\mu}|^2 + \boldsymbol{\Psi}^{\mathrm{T}}\left(i\not{D} + \mathcal{M}\right)\boldsymbol{\Psi}\right\} \tag{108}$$

for a while.

4.5 *Chiral anomaly on the graph*

We next consider the WT identity corresponding to the $U(1)_A$ symmetry. To this end, we consider the local $U(1)_A$ transformation

$$\eta^v \to e^{-i\theta_A^v}\eta^v, \qquad \lambda^e \to e^{i\theta_A^e}\lambda^e, \qquad \chi^f \to e^{-i\theta_A^f}\chi^f. \tag{109}$$

This local transformation is not the symmetry of the theory in general, but it makes the action invariant if the transformation is global (independent of the positions), namely $\theta_A^v = \theta_A^e = \theta_A^f$. We are now dealing with the graph Γ and the dual graph $\check{\Gamma}$ on an equal footing, where one edge is shared by two vertices and two faces. To respect this structure, we take the transformation parameters θ_A^e of the edge e to be the average of the transformation parameters of the vertices θ_A^v and faces θ_A^f,

$$\theta_A^e = \frac{1}{4}\left(\theta_A^{s(e)} + \theta_A^{t(e)} + \theta_A^{f_+(e)} + \theta_A^{f_-(e)}\right), \tag{110}$$

where $s(e)$, $t(e)$, and $f_\pm(e)$ are defined in Sect. 3.1. Then, the infinitesimal transformation of the action becomes

$$\delta S = \sum_{e\in E}\left\{\left(L^e{}_v\theta_A^v\right)J_e^{(V)} + \left(\check{L}^e{}_f\theta_A^f\right)J_e^{(F)} + \left(\left(K^e{}_v\theta_A^v\right) - \left(\check{K}^e{}_f\theta_A^f\right)\right)G_e\right\}, \tag{111}$$

where K and $\check{K}$ are the matrices given by Eqs. (48) and (51), respectively, and

$$J_e^{(V)} \equiv \frac{i}{g^2}\left(-\bar{\phi}^{t(e)}\phi^{s(e)} + \bar{\phi}^{s(e)}\phi^{t(e)} + \frac{1}{2}\lambda_e\sum_{v\in V}K^e{}_v\eta^v\right), \tag{112}$$

$$J_e^{(F)} \equiv \frac{i}{2g^2}\lambda_e\sum_{f\in F}\check{K}^e{}_f\hat{\chi}^f, \tag{113}$$

$$G_e \equiv \frac{i}{4g^2}\lambda_e\left(\sum_{v\in V}\left(L^e{}_v\eta^v\right) - \sum_{f\in F}\left(\check{L}^e{}_f\hat{\chi}^f\right)\right), \tag{114}$$

which are defined on each edge $e \in E$ and thus the index e is not contracted.

Recalling that the mass terms in Eq. (106) effectively supply all the fermion zero modes to the integration, we have also to evaluate the transformation of the integral measure $d\mathcal{B}d\mathcal{F}d\mathcal{F}_0$ and the inserted fermion zero modes. The infinitesimal transformation of the measure becomes

$$d\mathcal{B}d\mathcal{F}d\mathcal{F}_0 \to \left(1 + \sum_v\left(i\theta_A^v\right)\left(1 - \tfrac{1}{4}\deg(v)\right) + \sum_f\left(i\theta_A^f\right)\left(1 - \tfrac{1}{4}\deg(f)\right)\right)d\mathcal{B}d\mathcal{F}d\mathcal{F}_0, \tag{115}$$

and that of each fermion zero mode is

$$\eta_0 \to \eta_0 - i\sum_{v\in V}\theta_A^v\left(\boldsymbol{v}_0\right)_v\eta^v, \quad \chi_0 \to \chi_0 - i\sum_{f\in F}\theta_A^f\left(\boldsymbol{u}_0\right)_f\hat{\chi}^f, \quad \lambda_0^I \to \lambda_0^I + i\sum_{e\in E}\theta_A^d\left(\boldsymbol{e}_0^I\right)_e\lambda^e. \tag{116}$$

So, the zero mode integral is evaluated as

$$\int d\mathcal{F}_0\,\delta\left(\eta_0\chi_0\prod_{I=1}^{2h}\lambda_0^I\right)=\sum_{v\in V}\left(i\theta_A^v\right)\left(-(\boldsymbol{v}_0)_v^2+\frac{1}{4}\sum_{I=1}^{2h}\sum_{e\in E}K^e{}_v\left(\boldsymbol{e}_0^I\right)_e^2\right)$$
$$+\sum_{f\in F}\left(i\theta_A^f\right)\left(-(\boldsymbol{u}_0)_f^2+\frac{1}{4}\sum_{I=1}^{2h}\sum_{e\in E}\check{K}^e{}_f\left(\boldsymbol{e}_0^I\right)_e^2\right). \tag{117}$$

Combining Eqs. (111) and (117), we obtain the identities

$$\left\langle\sum_{e\in E}\left(L^e{}_vJ_e^{(V)}+K^e{}_vG_e\right)\right\rangle=-\left(1-\tfrac{1}{4}\deg(v)\right)+\left((\boldsymbol{v}_0)_v^2-\frac{1}{4}\sum_{I=1}^{2h}\sum_{e\in E}K^e{}_v\left(\boldsymbol{e}_0^I\right)_e^2\right), \tag{118}$$

$$\left\langle\sum_{e\in E}\left(\check{L}^e{}_fJ_e^{(F)}-\check{K}^e{}_fG_e\right)\right\rangle=-\left(1-\tfrac{1}{4}\deg(f)\right)+\left((\boldsymbol{u}_0)_f^2-\frac{1}{4}\sum_{I=1}^{2h}\sum_{e\in E}\check{K}^e{}_f\left(\boldsymbol{e}_0^I\right)_e^2\right) \tag{119}$$

on each $v\in V$ and $f\in F$. These identities are the local WT identities corresponding to Eq. (41) in the continuous theory. Note that we have two local WT identities for the single $U(1)_A$ symmetry because we are considering the graph and the dual graph at the same time: The transformation parameters θ_A^v and θ_A^f can be assigned independently on the vertices of the graph and the dual graph, respectively.

Interestingly, the quantities $1-\deg(v)/4$ and $1-\deg(f)/4$ appearing in the first parentheses of the right-hand sides correspond to the scalar curvature of the continuum geometry. We can justify this because they can be regarded as the deficit angle, which is proportional to the scalar curvature in two-dimensional geometry. To see this, suppose that all the faces are regular n-polygons of the same size. In this case $\deg(f)=n$ and the deficit angle around the vertex v is given by $\theta_v=2\pi\left(1-\frac{n-2}{2n}\deg(v)\right)$. Then, the average of the quantities around a vertex v becomes the deficit angle as described,

$$1-\tfrac{1}{4}\deg(v)+\sum_{f\in F_v}\frac{1}{\deg(f)}\left(1-\tfrac{1}{4}\deg(f)\right)=\frac{\theta_v}{2\pi}, \tag{120}$$

where F_v denotes the faces touching at the vertex v.

The second parentheses on the right-hand sides of Eqs. (118) and (119) are the contribution of the inserted fermion zero modes, which are necessary so that these identities are consistent. This is because, if we take summation over all the vertices of Eq. (118) and all the faces of Eq. (119) followed by summing these two identities, the terms with G_e trivially cancel and the remaining terms $\sum_{v,e}L^e{}_vJ_e^{(V)}$ and $\sum_{f,e}\check{L}^e{}_fJ_e^{(F)}$ vanish because of the structure of the matrices L and $\check{L}$. This corresponds to the integration over a total derivative vanishing in the continuous theory. On the other hand, after the same operation the first term of the right-hand side gives

$$-n_V-n_F+\frac{1}{4}\sum_v\deg(v)-\frac{1}{4}\sum_f\deg(f)=-n_V-n_F+n_E=-\chi_h, \tag{121}$$

which is a reproduction of the anomalous WT identity in Eq. (42) in the continuous theory with $G=U(1)$. However, if the second terms of the right-hand sides are absent, we obtain an inconsistent expression unless $\chi_h=0$ because the left-hand side vanishes. The second terms cure the situation such that

$$\sum_{v\in V}\left((\boldsymbol{v}_0)_v^2-\frac{1}{4}\sum_{I=1}^{2h}\sum_{e\in E}K^e{}_v\left(\boldsymbol{e}_0^I\right)_e^2\right)+\sum_{f\in F}\left((\boldsymbol{u}_0)_f^2-\frac{1}{4}\sum_{I=1}^{2h}\sum_{e\in E}\check{K}^e{}_f\left(\boldsymbol{e}_0^I\right)_e^2\right)=2-2h=\chi_h, \tag{122}$$

which cancels the contribution from the first terms in Eq. (121). This is consistent with the fact that the left-hand side vanishes.

5. Localization in the Abelian theory

5.1 *Saddle point equation*

We now apply the localization method to perform the path integral of the Abelian theory exactly.

Let $f[X]$ be a Q-closed operator. Recalling that the action is written in the Q-exact form such that $S = Q\Xi$, we see that the integration

$$\langle f[X]\rangle_t \equiv \int dX\, f[X] e^{-tS} \tag{123}$$

is independent of t. If we differentiate it by t, we obtain the vev of a Q-exact operator which vanishes at a supersymmetric vacuum:

$$\frac{\partial}{\partial t}\langle f[X]\rangle_t = -\langle Q(f[X]\,\Xi)\rangle_t = 0. \tag{124}$$

The path integral is localized at the saddle points in the limit of $t \to \infty$. Thus, we can evaluate the vev of a Q-closed operator, which includes the partition function itself, exactly by the saddle point approximation of the Abelian theory.

From the bosonic action in Eq. (73), we can see that the saddle points are given by

$$L\boldsymbol{\phi} = 0, \qquad \boldsymbol{\mu} = 0. \tag{125}$$

On the connected graph, the former equation always has the solution

$$\boldsymbol{\phi} = \phi_0 \boldsymbol{v}_0, \tag{126}$$

where $\phi_0 \in \mathbb{C}$ and $\boldsymbol{v}_0$ is the zero mode of L given by Eq. (46). We then expand the scalar fields around the saddle point as

$$\boldsymbol{\phi} = \phi_0 \boldsymbol{v}_0 + \frac{1}{\sqrt{t}}\tilde{\boldsymbol{\phi}}, \qquad \bar{\boldsymbol{\phi}} = \bar{\phi}_0 \boldsymbol{v}_0 + \frac{1}{\sqrt{t}}\tilde{\bar{\boldsymbol{\phi}}}, \tag{127}$$

where we have rescaled the fluctuation by $1/\sqrt{t}$ for later purposes.

For the moment map $\mu(P^f)$, the latter saddle point equation just means $P^f = 1$. Since the plaquette variable is given by

$$P^f = \exp\left\{ i L^{\mathrm{T}f}{}_e A^e \right\}, \tag{128}$$

the moment map constraint is solved by

$$\check{L}^{\mathrm{T}f}{}_e \hat{A}^e = 2\pi k^f, \tag{129}$$

where k^f are integers. As for the scalar fields, we expand the gauge field around the fixed point as

$$\boldsymbol{A} = \hat{\boldsymbol{A}} + \frac{1}{\sqrt{t}}\tilde{\boldsymbol{A}}. \tag{130}$$

In particular, around the fix points the plaquette variable behaves approximately as

$$\boldsymbol{\mu} \sim \frac{1}{\sqrt{t}}\check{L}^{\mathrm{T}}\tilde{\boldsymbol{A}} \tag{131}$$

up to a linear order of fluctuation $\tilde{\boldsymbol{A}}$. Then, the face part of the bosonic action around the saddle point becomes

$$\boldsymbol{Y}^{\mathrm{T}} \cdot \left(\boldsymbol{Y} - \frac{2}{\sqrt{t}}\check{L}^{\mathrm{T}}\tilde{\boldsymbol{A}} \right). \tag{132}$$

Looking at this expression, we see that the trace mode in the auxiliary field $\boldsymbol{Y}$ is decoupled from the gauge field at the saddle point. We then separate it from the others as

$$\boldsymbol{Y} = \frac{1}{\sqrt{t}}\left(Y_0\boldsymbol{u}_0 + \tilde{\boldsymbol{Y}}\right) \tag{133}$$

and rewrite Eq. (132) as

$$\frac{1}{t}\left\{Y_0^2 + \tilde{\boldsymbol{Y}}^{\mathrm{T}}\cdot\left(\tilde{\boldsymbol{Y}} - 2\check{L}\tilde{\boldsymbol{A}}\right)\right\}. \tag{134}$$

Note that we have also included the factor $1/\sqrt{t}$ in Y_0 because it is not the zero mode in the action but is just a free mode, as shown above.

After integrating out $\tilde{\boldsymbol{Y}}$, the 1-loop effective bosonic action becomes

$$S_{\mathrm{B}}^{\text{1-loop}} \equiv \lim_{t\to\infty} tS_{\mathrm{B}} = \frac{1}{2g^2}\left\{-Y_0^2 + \tilde{\bar{\boldsymbol{\phi}}}^T\Delta_V\tilde{\boldsymbol{\phi}} + \tilde{\boldsymbol{A}}^{\mathrm{T}}\check{L}\check{L}^{\mathrm{T}}\tilde{\boldsymbol{A}}\right\}. \tag{135}$$

We can ignore the first term in the present localization argument, since the integral of Y_0 is just Gaussian (by a rotation $Y_0 \to iY_0$) and irrelevant if any operator coupled with $\boldsymbol{Y}$ is not inserted. However, we will see later that the existence of Y_0 becomes important when inserting suitable operators including the auxiliary field.

For the fermions, we expand the fields around the fermion zero modes (if they exist) as

$$\boldsymbol{\eta} = \eta_0\boldsymbol{v}_0 + \frac{1}{\sqrt{t}}\tilde{\boldsymbol{\eta}}, \qquad \boldsymbol{\chi} = \chi_0\boldsymbol{u}_0 + \frac{1}{\sqrt{t}}\tilde{\boldsymbol{\chi}}, \qquad \boldsymbol{\lambda} = \sum_{I=1}^{2h}\lambda_0^I\boldsymbol{e}_0^I + \frac{1}{\sqrt{t}}\tilde{\boldsymbol{\lambda}}. \tag{136}$$

Then, the 1-loop effective action for the fermions reduces to

$$S_{\mathrm{F}}^{\text{1-loop}} \equiv \lim_{t\to\infty} tS_{\mathrm{F}} = -\frac{1}{g^2}\left\{\tilde{\boldsymbol{\eta}}^{\mathrm{T}}L^{\mathrm{T}}\tilde{\boldsymbol{\lambda}} + \tilde{\boldsymbol{\chi}}^{\mathrm{T}}\check{L}^{\mathrm{T}}\tilde{\boldsymbol{\lambda}}\right\}. \tag{137}$$

Note here that the fermion zero modes do not appear at all in the effective action since they are defined as the kernels of L and $\check{L}$.

For the inserted operator $f[X]$, by inserting the expansion in Eqs. (127) and (136), we obtain

$$\lim_{t\to\infty} f[X] = f[X_0], \tag{138}$$

where X_0 is the collective expression of the variables of the saddle points. Therefore, in evaluating the integration we have only to consider the inserted operator only when integrating over X_0.

5.2 *Gauge fixing and the 1-loop determinant*

The gauge transformation of the edge variable A^e is given by

$$\boldsymbol{A}' = \boldsymbol{A} - L\boldsymbol{\xi}, \tag{139}$$

where $\boldsymbol{\xi} \in \mathcal{V}_V$ is a gauge transformation parameter. We can see immediately (the exponent of) the plaquette variable

$$\boldsymbol{P} = \exp\left[i\check{L}^{\mathrm{T}}\boldsymbol{A}\right] \tag{140}$$

is invariant under this transformation because of the orthogonality of the incidence matrices in Eq. (56). This gauge invariance still keeps in the 1-loop effective action of Eqs. (135) and (137).

To proceed with the quantization (path integral) of the 1-loop effective theory, we introduce a gauge-fixing condition for the fluctuations

$$L^{\mathrm{T}}\tilde{\boldsymbol{A}} = 0, \tag{141}$$

which is an analogy with the Lorentz gauge in the continuous theory.

Introducing the Faddeev–Popov (FP) ghosts $(\boldsymbol{c}, \bar{\boldsymbol{c}})$ and the Nakanishi–Lautrup (NL) field $\boldsymbol{B}$ defined on V that obey the Becchi–Rouet–Stora–Tyutin (BRST) transformations

$$\delta_B \boldsymbol{c} = 0, \qquad \delta_B \bar{\boldsymbol{c}} = 2\boldsymbol{B}, \qquad \delta_B \boldsymbol{B} = 0, \tag{142}$$

the gauge-fixing and FP term is written by a BRST exact form,

$$S_{\mathrm{GF+FP}} = -\frac{1}{4g^2}\delta_B\left\{\bar{\boldsymbol{c}}^{\mathrm{T}} \cdot \left(\boldsymbol{B} - 2L^{\mathrm{T}}\tilde{\boldsymbol{A}}\right)\right\} = \frac{1}{2g^2}\left\{\bar{\boldsymbol{c}}^{\mathrm{T}}\Delta_V \boldsymbol{c} - \boldsymbol{B}^{\mathrm{T}} \cdot \left(\boldsymbol{B} - 2L^{\mathrm{T}}\tilde{\boldsymbol{A}}\right)\right\}, \tag{143}$$

where $\Delta_V = L^{\mathrm{T}}L$ and we have used the BRST transformation of the gauge field,

$$\delta_B \tilde{\boldsymbol{A}} = -L\boldsymbol{c}. \tag{144}$$

Combining the original action and gauge-fixing terms, we obtain the total action

$$\begin{aligned} S' &= S_B^{\text{1-loop}} + S_F^{\text{1-loop}} + S_{\mathrm{GF+FP}} \\ &= \frac{1}{2g^2}\Big\{\tilde{\bar{\boldsymbol{\phi}}}^{\mathrm{T}}\Delta_V\tilde{\boldsymbol{\phi}} + \tilde{\boldsymbol{A}}^{\mathrm{T}}\check{L}\check{L}^{\mathrm{T}}\tilde{\boldsymbol{A}} - 2\tilde{\boldsymbol{\eta}}^{\mathrm{T}}L^{\mathrm{T}}\tilde{\boldsymbol{\lambda}} - 2\tilde{\boldsymbol{\chi}}^{\mathrm{T}}\check{L}^{\mathrm{T}}\tilde{\boldsymbol{\lambda}} \\ &\qquad + \bar{\boldsymbol{c}}^{\mathrm{T}}\Delta_V\boldsymbol{c} - \boldsymbol{B}^{\mathrm{T}} \cdot \left(\boldsymbol{B} - 2L^{\mathrm{T}}\tilde{\boldsymbol{A}}\right)\Big\}. \end{aligned} \tag{145}$$

After eliminating the NL field $\boldsymbol{B}$, we get

$$S' = \frac{1}{2g^2}\Big\{\tilde{\bar{\boldsymbol{\phi}}}^{\mathrm{T}}\Delta_V\tilde{\boldsymbol{\phi}} + \bar{\boldsymbol{c}}^{\mathrm{T}}\Delta_V\boldsymbol{c} + \tilde{\boldsymbol{A}}^{\mathrm{T}}\Delta_E\tilde{\boldsymbol{A}} - 2\tilde{\boldsymbol{\eta}}^{\mathrm{T}}L^{\mathrm{T}}\tilde{\boldsymbol{\lambda}} - 2\tilde{\boldsymbol{\chi}}^{\mathrm{T}}\check{L}^{\mathrm{T}}\tilde{\boldsymbol{\lambda}}\Big\}, \tag{146}$$

where $\Delta_E = LL^{\mathrm{T}} + \check{L}\check{L}^{\mathrm{T}}$.

From this quadratic 1-loop effective action, we can perform the path integral for the non-zero modes explicitly; the 1-loop determinant becomes

$$(\text{1-loop det}) = \frac{\det'\Delta_V}{\det'\Delta_V}\frac{\left(\det'\Delta_V\det'\Delta_F\det'\Delta_E\right)^{1/4}}{\sqrt{\det'\Delta_E}} = \left(\frac{\det'\Delta_V\det'\Delta_F}{\det'\Delta_E}\right)^{1/4} = 1 \tag{147}$$

up to an irrelevant sign factor due to the Pfaffian from the fermions, where the $'$ denotes that the zero modes are omitted in the evaluation of the determinant, and we have used the fact that the non-zero eigenvalues of Δ_E are identical to those of Δ_V and Δ_F:

$$\mathrm{Spec}'\,\Delta_V \oplus \mathrm{Spec}'\,\Delta_F = \mathrm{Spec}'\,\Delta_E. \tag{148}$$

Since the zero modes are dropped from the 1-loop effective actions $S_{\mathrm{B}}^{\text{1-loop}}$ and $S_{\mathrm{F}}^{\text{1-loop}}$, there exist residual integrals over the zero modes after integrating out the non-zero modes; namely, the vev reduces to the integral over the zero modes,

$$\langle f[X]\rangle = \mathcal{N}\int d\phi_0 d\bar{\phi}_0 dY_0\left(\prod_{I=1}^{2h} d\lambda_0^{2h-I+1}\right) d\chi_0 d\eta_0\, f[X_0]e^{\frac{1}{2g^2}Y_0^2}, \tag{149}$$

up to an irrelevant normalization constant $\mathcal{N}$ of the path integral measure. Note that this reduction works only when $f[X]$ is Q-closed. In particular, by setting $f[X] = 1$, we again see that the partition function vanishes due to the Grassmann integral, as pointed out in the previous subsection.

5.3 *Compensating for the zero modes*

As discussed above, the vev of the operator reduces to the residual integral over the zero modes after integrating out the non-zero modes. Therefore, so that the operator has a non-trivial vev, we need to insert at least suitable fermion zero modes. In the previous subsection we simply added the mass term of the fermion zero modes in Eq. (106), but such an operator that is *not*

Q-invariant is not appropriate in the present situation. Instead, we consider here Q-closed operators in order not to spoil the above localization argument. Such Q-closed operators behave as mass terms for the fermions, namely an exponential of the fermion bi-linear term, including all the fermion zero modes. We call this kind of physical operator the compensator in the following [54].

First, we define a Q-exact operator which includes $\boldsymbol{\eta}$ and $\boldsymbol{\chi}$,

$$\mathcal{O}_{\eta\chi} \equiv Q\big(\chi_f \bar{\mathcal{W}}'(\bar{\phi}^f)\big) = Y_f \bar{\mathcal{W}}'(\bar{\phi}^f) + 2\bar{\mathcal{W}}''(\bar{\phi}_f)\eta_f \chi^f, \tag{150}$$

where $\bar{\mathcal{W}}'(\bar{\phi}^f)$ is an analytic function of $\bar{\phi}^f$ only.[5] If we insert the exponential of this operator into the path integral, all the fields are effectively replaced by their zero modes as mentioned in the previous subsection and the inserted operator reduces to

$$e^{-\frac{1}{g^2}\mathcal{O}_{\eta\lambda}} \to -\frac{2}{g^2}\bar{\mathcal{W}}''(\bar{\phi}_0)\eta_0\chi_0 e^{-\frac{1}{g^2}Y_0\bar{\mathcal{W}}'(\bar{\phi}_0)} \tag{151}$$

in the integrand. This compensates for the zero modes of $\boldsymbol{\eta}$ and $\boldsymbol{\chi}$ as expected.

We next define an operator which includes bi-linear terms of $\boldsymbol{\lambda}$ to compensate for the zero-mode integral of λ_0^I. As one of the candidates of the fermion bi-linear term, we now consider an operator

$$\frac{1}{2}\boldsymbol{\lambda}^{\mathrm{T}}\Omega\boldsymbol{\lambda}, \tag{152}$$

where Ω is an anti-symmetric $n_E \times n_E$ matrix, namely $\Omega^{\mathrm{T}} = -\Omega$. The supercharge Q acts on this by

$$\frac{1}{2}Q\left(\boldsymbol{\lambda}^{\mathrm{T}}\Omega\boldsymbol{\lambda}\right) = -\boldsymbol{\phi}^{\mathrm{T}}L^{\mathrm{T}}\Omega\boldsymbol{\lambda}. \tag{153}$$

On the other hand, we consider the operator piece

$$\check{\boldsymbol{\phi}}^{\mathrm{T}} \cdot \check{L}^{\mathrm{T}}\boldsymbol{A}, \tag{154}$$

where $\check{\boldsymbol{\phi}}$ is a dual scalar field on the face F, which is linearly constructed from the original scalar field $\boldsymbol{\phi}$ on V via

$$\check{\boldsymbol{\phi}} = M\boldsymbol{\phi}, \tag{155}$$

where M is an $n_F \times n_V$ matrix. Note here that there are multiple candidates for M; typically, $\check{\phi}^f$ is determined by ϕ^v on the representative point at the boundary of the face.

Substituting Eq. (155) into Eq. (154) and applying the Q-transformation, we find that

$$Q\big(\boldsymbol{\phi}^{\mathrm{T}}M^{\mathrm{T}}\check{L}^{\mathrm{T}}\boldsymbol{A}\big) = \boldsymbol{\phi}^{\mathrm{T}}M^{\mathrm{T}}\check{L}^{\mathrm{T}}\boldsymbol{\lambda}. \tag{156}$$

Then, using Eqs. (153) and (156), we see that the combined operator

$$\mathcal{O}_{\lambda\lambda} = \check{\boldsymbol{\phi}}^{\mathrm{T}}\check{L}^{\mathrm{T}}\boldsymbol{A} + \tfrac{1}{2}\boldsymbol{\lambda}^{\mathrm{T}}\Omega\boldsymbol{\lambda} \tag{157}$$

is Q-closed if there is the following relation between the matrices:

$$\Omega L + \check{L}M = 0. \tag{158}$$

So, the operator $\mathcal{O}_{\lambda\lambda}$ could become a non-trivial observable. We note here that the operator in Eq. (157) is Q-closed but is *not* Q-exact.

As well as $\mathcal{O}_{\eta\chi}$, if we insert $e^{-i\mathcal{O}_{\lambda\lambda}}$ in the path integral it reduces to an integrand of the zero modes as a summation over the saddle points,

$$e^{-i\mathcal{O}_{\lambda\lambda}} \to \sum_{k\in\mathbb{Z}} e^{-i\left(2\pi k\phi_0 - \frac{1}{2}\lambda_0^I\left(\boldsymbol{e}_0^I\right)^{\mathrm{T}}\Omega\boldsymbol{e}_0^J\lambda_0^J\right)} = \mathcal{C}\left(\prod_{I=1}^{2h}\lambda_0^I\right)\sum_{n\in\mathbb{Z}}\delta(\phi_0 - n), \tag{159}$$

[5] Since we can regard $\bar{\mathcal{W}}$ as the superpotential, the first and second derivatives of $\bar{\mathcal{W}}$ appear here.

where $\mathcal{C}$ is an irrelevant constant and we have used that $\boldsymbol{A}$ satisfies

$$\check{L}^{\mathrm{T}f}{}_{e}\hat{A}^{e} = 2\pi k^{f} \tag{160}$$

at the saddle point with the total magnetic flux $k = \sum_{f\in F} k^f$, and the Poisson summation formula $\sum_{k\in\mathbb{Z}} e^{2\pi i k x} = \sum_{n\in\mathbb{Z}} \delta(x-n)$. This compensates for the zero modes of $\boldsymbol{\lambda}$ as expected.

Then, if we insert the compensator $e^{\frac{1}{g^2}\mathcal{O}_{\eta\chi}} e^{-i\mathcal{O}_{\lambda\lambda}}$ in the path integral, we can compensate for all the fermion zero modes and make the integration well-defined. However, this is not the only effect of the compensator: it can handle not only fermion zero modes but also the boson zero modes at the same time.

To see this, let us consider the vev

$$\left\langle f[\boldsymbol{\phi}]\, e^{-\frac{1}{2g^2}\mathcal{O}_{\eta\chi}}\, e^{-i\mathcal{O}_{\lambda\lambda}} \right\rangle \tag{161}$$

using the localization method, where $f[\boldsymbol{\phi}]$ is an analytic function constructed by $\boldsymbol{\phi}$ only and trivially Q-closed. Using Eq. (149) with Eqs. (151) and (159), we obtain

$$\begin{aligned}
\left\langle f[\boldsymbol{\phi}]\, e^{-\frac{1}{2g^2}\mathcal{O}_{\eta\chi}}\, e^{-i\mathcal{O}_{\lambda\lambda}} \right\rangle &= -\frac{2}{g^2}\mathcal{N}\mathcal{C} \int \left(\prod_{I=1}^{2h} d\lambda_0^{2h-I+1} \right) d\chi_0 d\eta_0 \left(\eta_0 \chi_0 \prod_{I=1}^{2h} \lambda_0^I \right) \\
&\quad \times \int d\phi_0 d\bar{\phi}_0 dY_0\, \bar{\mathcal{W}}''(\bar{\phi}_0) f(\phi_0) e^{\frac{1}{2g^2}(Y_0^2 - 2\bar{\mathcal{W}}'(\bar{\phi}_0)Y_0)} \sum_{n\in\mathbb{Z}} \delta(\phi_0 - n) \\
&= -\frac{\sqrt{8\pi}}{g}\mathcal{N}\mathcal{C} \sum_{n\in\mathbb{Z}} f(n),
\end{aligned} \tag{162}$$

where, after eliminating Y_0, the integration over $\bar{\phi}_0$ becomes just a Gaussian integral by changing the variable from $\bar{\phi}_0$ to $\bar{\mathcal{W}}'(\bar{\phi}_0)$. This result of course holds for $f[X] = 1$, and thus the partition function is also regularized by inserting the compensators.[6] In this sense, the compensators give a regularization of the zero modes in the Abelian theory.

6. Non-Abelian gauge theory

In this section we generalize our discussion to the non-Abelian gauge group $G = U(N)$. The bosonic variables (fields) on V, E, and F are denoted by Φ^v, U^e, and Y^f, respectively. Also, the fermionic fields η^v, λ^e, and χ^f exist on V, E, and F, respectively. For the non-Abelian gauge group, all the fields except for U^e are extended to the adjoint representation of $U(N)$, namely $N \times N$ matrices, while the edge variables U^e are $N \times N$ unitary matrices.

The supersymmetry transformation is given by

$$\begin{aligned}
&Q\Phi^v = 0, && \\
&Q\bar{\Phi}^v = 2\eta^v, && Q\eta^v = \tfrac{i}{2}[\Phi^v, \bar{\Phi}^v], \\
&QU^e = i\lambda^e U^e, && Q\lambda^e = -L_U{}^e{}_v \Phi^v + i\lambda^e\lambda^e, \\
&QY^f = i[\check{\Phi}^f, \chi^f], && Q\chi^f = Y^f,
\end{aligned} \tag{163}$$

where L_U is defined as a gauge covariant incidence matrix,

$$L_U{}^e{}_v \Phi^v \equiv U^e \Phi^{t(e)} U^{e\dagger} - \Phi^{s(e)}, \tag{164}$$

and f of $\check{\Phi}^f$ denotes the representative vertex of the face f.

It is sometimes useful to define

$$\Lambda^e \equiv \lambda^e U^e. \tag{165}$$

[6] We also have to regularize $\sum_{n\in\mathbb{Z}} 1$ in some way, though.

The supersymmetry transformations for U^e and Λ^e become

$$QU^e = i\Lambda^e, \qquad Q\Lambda^e = -(U^e\Phi^{t(e)} - \Phi^{s(e)}U^e). \tag{166}$$

We can construct the supersymmetric action in the Q-exact form

$$S = -\frac{1}{2g^2} Q\,\mathrm{Tr}\left\{\frac{i}{2}\eta_v[\Phi^v, \bar{\Phi}^v] + (\bar{\Phi}_{t(e)}U_e^\dagger - U_e^\dagger\bar{\Phi}_{s(e)})\Lambda^e + \chi_f\big(Y^f - 2\mu(P^f)\big)\right\}. \tag{167}$$

The moment map $\mu(P^f)$ in the action is a function of the plaquette variable on each face labeled by f, which is defined by an ordered product around a face,

$$P^f \equiv (U^{e_1})^{\check{L}^{\mathrm{T}f}{}_{e_1}} (U^{e_2})^{\check{L}^{\mathrm{T}f}{}_{e_2}} \cdots (U^{e_n})^{\check{L}^{\mathrm{T}f}{}_{e_n}}, \tag{168}$$

where $\{e_1, e_2, \ldots, e_n\}$ are edges that surround the face f in this order. We choose the function $\mu(P^f)$ so that it has a unique vacuum at $P^f = 1$ and asymptotically behaves as the field strength of the gauge field around the vacuum in order to induce the gauge kinetic term after eliminating the auxiliary field Y^f [5,50].

Using the supersymmetry transformations, the bosonic part becomes

$$S_{\mathrm{B}} = \frac{1}{2g^2}\mathrm{Tr}\left\{\frac{1}{4}[\Phi^v, \bar{\Phi}^v]^2 + |U^e\Phi^{t(e)} - \Phi^{s(e)}U^e|^2 - Y_f\big(Y^f - 2\mu(P^f)\big)\right\}, \tag{169}$$

and the fermionic part becomes

$$\begin{aligned} S_F = -\frac{1}{2g^2}\mathrm{Tr}\big\{&-i\eta_v[\Phi^v, \eta^v] + 2(\eta_{t(e)}U_e^\dagger - U_e^\dagger\eta_{s(e)})\Lambda^e - i(\bar{\Phi}_{t(e)}U_e^\dagger\Lambda_e U_e^\dagger \\ &- U_e^\dagger\Lambda_e U_e^\dagger\bar{\Phi}_{s(e)})\Lambda^e - i\chi_f[\check{\Phi}^f, \chi^f] + 2\chi_f Q\mu(P^f)\big\}. \end{aligned} \tag{170}$$

Using the Q-exact action, the partition function of the non-Abelian gauge theory is given by

$$Z = \int \prod_{v\in V}\mathcal{D}\Phi^v\mathcal{D}\bar{\Phi}^v\mathcal{D}\eta^v \prod_{e\in E}\mathcal{D}U^e\mathcal{D}\lambda^e \prod_{f\in F}\mathcal{D}Y^f\mathcal{D}\chi^f\, e^{-S}. \tag{171}$$

Under the $U(1)_A$ rotation, each field transforms as

$$\begin{aligned} &\Phi^v \to e^{2i\theta_A}\Phi^v, \quad &&\bar{\Phi}^v \to e^{-2i\theta_A}\bar{\Phi}^v, \quad &&U^e \to U^e, \quad &&Y^f \to Y^f, \\ &\eta^v \to e^{-i\theta_A}\eta^v, &&\lambda^e \to e^{i\theta_A}\lambda^e, &&\chi^f \to e^{-i\theta_A}\chi^f. \end{aligned} \tag{172}$$

Then, the path integral measure of the fermions has a $U(1)_A$ anomaly

$$\begin{aligned} \prod_{v\in V}\mathcal{D}\eta^v\prod_{e\in E}\mathcal{D}\lambda^e\prod_{f\in F}\mathcal{D}\chi^f &\to e^{i\dim U(N)\times(n_V - n_E + n_F)\theta_A}\prod_{v\in V}\mathcal{D}\eta^v\prod_{e\in E}\mathcal{D}\lambda^e\prod_{f\in F}\mathcal{D}\chi^f \\ &= e^{iN^2\chi_h\theta_A}\prod_{v\in V}\mathcal{D}\eta^v\prod_{e\in E}\mathcal{D}\lambda^e\prod_{f\in F}\mathcal{D}\chi^f. \end{aligned} \tag{173}$$

We will see later that this $U(1)_A$ anomaly essentially comes from the fermion zero modes.

With the usual localization arguments, we can show that the Q-exact action in Eq. (167) is independent of an overall coupling constant t of the rescaled action $S \to tS$. So, the saddle point approximation in the limit of $t \to \infty$ becomes exact and the path integral is localized at the saddle (fixed) points. From the bosonic part of the action S_{B}, we find that the saddle points (localization fixed points) are given by the equations

$$[\Phi^v, \bar{\Phi}^v] = 0, \tag{174}$$

$$L_{U^e{}_v}\Phi^v = 0, \tag{175}$$

$$\mu(P^f) = 0. \tag{176}$$

The first equation, Eq. (174), shows that Φ^v are diagonal. We denote this diagonal solution by

$$\hat{\Phi}^v = \mathrm{diag}(\hat{\phi}^{v,1}, \hat{\phi}^{v,2}, \ldots, \hat{\phi}^{v,N}). \tag{177}$$

Using this diagonal expression, we can solve the second equation, Eq. (175), by

$$\hat{\phi}^{t(e),\pi_e(i)} = \hat{\phi}^{s(e),i}, \tag{178}$$

$$U^e = \hat{U}^e \Pi^e, \tag{179}$$

where $\hat{U}^e$ is a diagonal matrix,

$$\hat{U}^e = \mathrm{diag}(\hat{U}^{e,1}, \hat{U}^{e,2}, \ldots, \hat{U}^{e,N}) \qquad (|\hat{U}^{e,i}| = 1), \tag{180}$$

and Π^e is a permutation matrix which represents the order-N permutation $\pi_e \in \mathfrak{S}_N$ on the edge e.

Since the permutation belongs to the Weyl group of $U(N)$, we can choose $\Pi^e = 1$ without loss of generality by using a gauge transformation. So the diagonal element of Φ^v on each vertex is written by a common diagonal element independent of v, that is,

$$\hat{\phi}^{v,i} = \phi_0^i, \tag{181}$$

which represents a "constant" zero mode.

Finally, Eq. (176) implies a constraint on $U^{e,i}$:

$$\prod_{e\in f} \left(\hat{U}^{e,i}\right)^{\check{L}^{\mathrm{T}f}{}_e} = 1, \tag{182}$$

for each f and i.

Now let us consider an effective action near the saddle point. We expand Φ^v and U^e around the solution to the saddle point equation as

$$\begin{aligned}\Phi^v &= \hat{\Phi} + \frac{1}{\sqrt{t}}\tilde{\Phi}^v,\\ U^e &= e^{\frac{i}{\sqrt{t}}\tilde{A}^e}\hat{U}^e \simeq \left(1 + \frac{i}{\sqrt{t}}\tilde{A}^e\right)\hat{U}^e,\end{aligned} \tag{183}$$

where $\hat{\Phi} = \mathrm{diag}(\phi_0^1, \phi_0^2, \ldots, \phi_0^N)$. All the other fields including the fermions are treated as fluctuations and rescaled by $1/\sqrt{t}$, and we omit the $\sim$for these fluctuations. Using the Cartan–Weyl basis (see Appendix B), the Cartan parts are written as

$$\hat{\Phi} = \phi_0^i \mathrm{H}_i, \qquad \hat{\bar{\Phi}} = \bar{\phi}_0^i \mathrm{H}_i, \qquad \hat{U}^e = \hat{U}^{e,i}\mathrm{H}_i, \tag{184}$$

and the fluctuations and fermions are expanded as follows:

$$\begin{array}{lll}\tilde{\Phi}^v = \tilde{\phi}^{v,i}\mathrm{H}_i + \tilde{\phi}^{v,\alpha}\mathrm{E}_\alpha, & \tilde{\bar{\Phi}}^v = \tilde{\bar{\phi}}^{v,i}\mathrm{H}_i + \tilde{\bar{\phi}}^{v,\alpha}\mathrm{E}_\alpha, & \tilde{A}^e = \tilde{A}^{e,i}\mathrm{H}_i + \tilde{A}^{e,\alpha}\mathrm{E}_\alpha,\\ \eta^v = \eta^{v,i}\mathrm{H}_i + \eta^{v,\alpha}\mathrm{E}_\alpha, & \chi^f = \chi^{f,i}\mathrm{H}_i + \chi^{f,\alpha}\mathrm{E}_\alpha, & \lambda^e = \lambda^{e,i}\mathrm{H}_i + \lambda^{e,\alpha}\mathrm{E}_\alpha,\end{array} \tag{185}$$

where the upper and lower indices of i and α are contracted.

Using these expansions, we find that

$$\begin{aligned}[\Phi^v, \bar{\Phi}^v] &= \frac{1}{\sqrt{t}}\left([\hat{\Phi}, \tilde{\bar{\Phi}}^v] + [\tilde{\Phi}^v, \hat{\bar{\Phi}}]\right) + \mathcal{O}(1/t), = \frac{1}{\sqrt{t}}\left(\alpha(\phi_0)\tilde{\bar{\phi}}^{v,\alpha} - \alpha(\bar{\phi}_0)\tilde{\phi}^{v,\alpha}\right)\mathrm{E}_\alpha + \mathcal{O}(1/t),\\ L_{U}{}^e{}_v\Phi^v &= \frac{1}{\sqrt{t}}\left(L^e{}_v\tilde{\phi}^{v,i}\mathrm{H}_i + L_{\hat{U}}{}^e{}_v\tilde{\phi}^{v,\alpha}\mathrm{E}_\alpha - i\alpha(\phi_0)\tilde{A}^{e,\alpha}\mathrm{E}_\alpha\right) + \mathcal{O}(1/t),\\ \mu(P^f) &= \frac{1}{\sqrt{t}}\left(\check{L}^{\mathrm{T}f}{}_e\tilde{A}^{e,i}\mathrm{H}_i + \check{L}^{\dagger}_{\hat{U}}{}^f{}_e\tilde{A}^{e,\alpha}\mathrm{E}_\alpha\right) + \mathcal{O}(1/t)\end{aligned} \tag{186}$$

up to the leading order, where

$$\alpha(\phi_0) \equiv \alpha_i \phi_0^i, \qquad \alpha(\bar{\phi}_0) \equiv \alpha_i \bar{\phi}_0^i. \tag{187}$$

When we expand the moment map $\mu(P^f)$, we require the covariant dual incidence matrix $\check{L}_{\hat{U}}^{\dagger}{}^{f}{}_{e}$, which is defined by

$$\delta\mu(P^f)\big|_{U^e=\hat{U}^e} = i\sum_{e\in f} \check{L}_{\hat{U}}^{\dagger}{}^{f}{}_{e}\delta A^e \equiv i\sum_{e\in f} \check{L}^{\dagger f}{}_{e}\hat{X}_e^f \delta A^e \hat{X}_e^{\dagger f}, \tag{188}$$

with

$$\hat{X}_{e_i}^f = \begin{cases} \hat{U}_{e_1}^{\check{L}_{e_1}^f}\hat{U}_{e_2}^{\check{L}_{e_2}^f}\cdots\hat{U}_{e_{i-1}}^{\check{L}_{e_{i-1}}^f} & \text{if } \check{L}^f{}_{e_i} = +1, \\ \hat{U}_{e_1}^{\check{L}_{e_1}^f}\hat{U}_{e_2}^{\check{L}_{e_2}^f}\cdots\hat{U}_{e_i}^{\check{L}_{e_i}^f} & \text{if } \check{L}^f{}_{e_i} = -1. \end{cases} \tag{189}$$

Using the above expansions up to quadratic order of fluctuations, we obtain the rescaled 1-loop effective bosonic action:

$$\begin{aligned} S_{\rm B}^{\text{1-loop}} \equiv \lim_{t\to\infty} tS_{\rm B} = \frac{1}{2g^2}\Bigg[&\sum_{i=1}^{N}\left\{|L^e{}_v\tilde{\phi}^{v,i}|^2 - Y_f^i(Y^{f,i} - 2\check{L}^{\mathrm{T}f}{}_e\tilde{A}^{e,i})\right\} \\ &+ \sum_{\alpha}\Bigg\{\frac{1}{4}\left|\alpha(\phi_0)\tilde{\bar{\phi}}^{v,\alpha} - \alpha(\bar{\phi}_0)\tilde{\phi}^{v,\alpha}\right|^2 + |L_{\hat{U}}{}^e{}_v\tilde{\phi}^{v,\alpha}|^2 + |\alpha(\phi_0)\tilde{A}^{e,\alpha}|^2 \\ &- Y_f^{-\alpha}(Y^{f,\alpha} - 2\check{L}_{\hat{U}}^{\dagger}{}^{f}{}_{e}\tilde{A}^{e,\alpha})\Bigg\}\Bigg]. \end{aligned} \tag{190}$$

Similarly, the fermionic part of the 1-loop effective action becomes

$$\begin{aligned} S_{\rm F}^{\text{1-loop}} \equiv \lim_{t\to\infty} tS_{\rm F} = -\frac{1}{2g^2}\Bigg[&\sum_{i=1}^{N}\left\{2\eta_v^i L^{\mathrm{T}v}{}_e\lambda^{e,i} + 2\chi_f^i\check{L}^{\mathrm{T}f}{}_e\lambda^{e,i}\right\} \\ &+ \sum_{\alpha}\Bigg\{2\eta_v^{-\alpha}L_{\hat{U}}^{\dagger}{}^{v}{}_{e}\lambda^{e,\alpha} + 2\chi_f^{-\alpha}\check{L}_{\hat{U}}^{\dagger}{}^{f}{}_{e}\lambda^{e,\alpha} \\ &- i\alpha(\phi_0)\eta_v^{-\alpha}\eta^{v,\alpha} - i\alpha(\phi_0)\chi_f^{-\alpha}\chi^{f,\alpha} + i\alpha(\bar{\phi}_0)\lambda_e^{-\alpha}\lambda^{e,\alpha}\Bigg\}\Bigg]. \end{aligned} \tag{191}$$

This effective action gives the same path integral as the original action owing to the Q-exactness of the action.

We first integrate over the components of the root vectors. To this end, we fix the gauge symmetry $U(1)^N$ in the 1-loop actions in Eqs. (190) and (191) by introducing the FP ghost $(c^{v,\alpha}, \bar{c}^{v,\alpha})$ and NL field $B^{v,\alpha}$. The corresponding BRST transformations are given by

$$\begin{aligned} &\delta_B c^{v,\alpha} = 0, && \delta_B \bar{c}^{v,\alpha} = 2B^{v,\alpha}, && \delta_B B^{v,\alpha} = 0, \\ &\delta_B\tilde{\phi}^{v,\alpha} = -i\alpha(\phi_0)c^{v,\alpha}, && \delta_B\tilde{\bar{\phi}}^{v,\alpha} = -i\alpha(\bar{\phi}_0)c^{v,\alpha}, && \\ &\delta_B\tilde{A}^{e,\alpha} = -L_{\hat{U}}{}^e{}_v c^{v,\alpha}, && && \end{aligned} \tag{192}$$

where we assume that the FP ghost and NL field are the same order in t as the fluctuations. We define the gauge-fixing function for the root vectors by

$$f^{v,\alpha} \equiv B^{v,\alpha} - 2L_{\hat{U}}^{\dagger}{}^{v}{}_{e}\tilde{A}^{e,\alpha} + i\alpha(\phi_0)\tilde{\bar{\phi}}^{v,\alpha} + i\alpha(\bar{\phi}_0)\tilde{\phi}^{v,\alpha}. \tag{193}$$

Then, the gauge-fixing and FP ghost term is given in the BRST exact form by

$$S^{\rm root}_{\rm GF+FP} = -\frac{1}{4g^2}\delta_B \sum_\alpha \bar{c}_v^{-\alpha} f^{v,\alpha}$$
$$= \frac{1}{2g^2}\sum_\alpha \left[-B_v^{-\alpha} f^{v,\alpha} + \bar{c}_v^{-\alpha}\left(\Delta_{\hat{U}}^{V\,v}{}_{v'} + |\alpha(\phi_0)|^2\delta^v{}_{v'}\right) c^{v',\alpha}\right], \tag{194}$$

where

$$\Delta_{\hat{U}}^{V\,v}{}_{v'} \equiv L^{\dagger}_{\hat{U}}{}^{v}{}_{e} L_{\hat{U}}{}^{e}{}_{v'}. \tag{195}$$

After eliminating the NL field $B^{v,\alpha}$, we get the action for $(\tilde{\phi}^{v,\alpha}, \tilde{\bar{\phi}}^{v,\alpha})$,

$$S^{\rm root}_{(\tilde{\phi},\tilde{\bar{\phi}})} = \frac{1}{2g^2}\sum_\alpha \tilde{\bar{\phi}}_v^{-\alpha}\left(\Delta_{\hat{U}}^{V\,v}{}_{v'} + |\alpha(\phi_0)|^2\delta^v{}_{v'}\right)\tilde{\phi}^{v',\alpha}, \tag{196}$$

whose 1-loop determinant is completely canceled with the contribution from the ghost part in Eq. (194).

In addition, integrating out the auxiliary field $Y^{f,\alpha}$, the action for the gauge boson reduces to

$$S^{\rm root}_{\tilde{A}} = \frac{1}{2g^2}\sum_\alpha \tilde{A}_e^{-\alpha}\left(\Delta_{\hat{U}}^{E\,e}{}_{e'} + |\alpha(\phi_0)|^2\delta^e{}_{e'}\right)\tilde{A}^{e',\alpha}, \tag{197}$$

where

$$\Delta_{\hat{U}}^{E\,e}{}_{e'} \equiv L_{\hat{U}}{}^{e}{}_{v} L^{\dagger}_{\hat{U}}{}^{v}{}_{e'} + \check{L}_{\hat{U}}{}^{e}{}_{v}\check{L}^{\dagger}_{\hat{U}}{}^{v}{}_{e'}. \tag{198}$$

Then we obtain the 1-loop determinant for the gauge boson $\tilde{A}^{e,\alpha}$,

$$\prod_{\alpha>0}\frac{1}{|\alpha(\phi_0)|^{2n_E^0}\det{}'\left(\Delta_{\hat{U}}^E + |\alpha(\phi_0)|^2\right)}, \tag{199}$$

where n_E^0 is the number of zero eigenstates for the edge Laplacian, and the $'$ on the determinant represents omission of the zero eigenvalues.

Next, let us consider the integral of the fermions. We need to take care with the Laplacian zero modes for the fermions, but we get the 1-loop determinant

$$\prod_{\alpha>0}\alpha(\phi_0)^{n_V^0+n_F^0}\alpha(\bar{\phi}_0)^{n_E^0}\left\{\det{}'\left(\Delta_{\hat{U}}^V + |\alpha(\phi_0)|^2\right)\det{}'\left(\Delta_{\hat{U}}^F + |\alpha(\phi_0)|^2\right)\det{}'\left(\Delta_{\hat{U}}^E + |\alpha(\phi_0)|^2\right)\right\}^{1/2}$$
$$= \prod_{\alpha>0}\alpha(\phi_0)^{n_V^0+n_F^0}\alpha(\bar{\phi}_0)^{n_E^0}\det{}'\left(\Delta_{\hat{U}}^E + |\alpha(\phi_0)|^2\right), \tag{200}$$

where we have used that the non-zero eigenvalues of $\Delta_{\hat{U}}^E$ are a combination of the non-zero eigenvalues of $\Delta_{\hat{U}}^V$ and $\Delta_{\hat{U}}^F$, namely[7]

$${\rm Spec}'\,\Delta_{\hat{U}}^V \oplus {\rm Spec}'\,\Delta_{\hat{U}}^F = {\rm Spec}'\,\Delta_{\hat{U}}^E. \tag{201}$$

Combining the 1-loop determinant of the bosons, Eq. (199), and fermions, Eq. (200), we finally obtain the total 1-loop determinant for the root vector components,

$$\prod_{\alpha>0}\alpha(\phi_0)^{n_V^0+n_F^0-n_E^0} = \prod_{\alpha>0}\alpha(\phi_0)^{\chi_h}, \tag{202}$$

[7]We can see that the condition in Eq. (182) guarantees the orthogonality like Eq. (56) for $L_{\hat{U}}$ and $\check{L}_{\hat{U}}$ in the concrete examples. See Appendix A.

where we have used the index theorem on the graph Laplacians as well as Abelian theory. Note here that the above 1-loop determinant has an anomaly phase under $U(1)_A$ symmetry as

$$\prod_{\alpha>0}\alpha(\phi_0)^{\chi_h} \to e^{iN(N-1)\chi_h\theta_A}\prod_{\alpha>0}\alpha(\phi_0)^{\chi_h}. \tag{203}$$

We next turn to the Cartan part of the fluctuations and fermions. The Cartan part is nothing but N copies of the Abelian theory discussed in Sect. 5. Introducing the FP ghost ($c^{v,i}$, $\bar{c}^{v,i}$), NL field $B^{v,i}$, and gauge-fixing function for the Cartan modes

$$f^{v,i} = B^{v,i} - 2L^{\mathrm{T}\,v}{}_e\tilde{A}^{e,i}, \tag{204}$$

the gauge-fixing term for the Cartan modes is given by

$$S^{\mathrm{Cartan}}_{\mathrm{GF+FP}} = -\frac{1}{4g^2}\delta_B\sum_{i=1}^N \bar{c}^i_v f^{v,i} = \frac{1}{2g^2}\sum_{i=1}^N\left[-B^i_v f^{v,i} + \bar{c}^i_v\Delta_V{}^v{}_{v'}c^{v',i}\right]. \tag{205}$$

We find that the 1-loop determinant of the bosons ($\tilde{\phi}^{v,i}$, $\tilde{\bar{\phi}}^{v,i}$) and ($c^{v,i}$, $\bar{c}^{v,i}$) cancel each other. After eliminating the auxiliary field $Y^{f,i}$ and NL field $B^{v,i}$, the integral of the gauge boson $\tilde{A}^{e,i}$ gives the 1-loop determinant

$$\frac{1}{\left(\det'\Delta_E\right)^N}. \tag{206}$$

This 1-loop determinant for the bosons cancels with the 1-loop determinant for the fermions,

$$\left(\det'\Delta_V\,\det'\Delta_F\,\det'\Delta_E\right)^{N/2}, \tag{207}$$

by using the same fact as Eq. (148) for the Cartan part.

Thus, we finally obtain the path integral measure over the zero modes in the Cartan subalgebra,

$$Z = \mathcal{N}\int\prod_{i=1}^N d\phi^i_0 d\bar{\phi}^i_0 d\,Y^i_0\left(\prod_{I=1}^{2h}d\lambda_0^{i,2h-I+1}\right)d\,\chi^i_0 d\eta^i_0\, e^{\frac{1}{2g^2}(Y^i_0)^2}\prod_{\alpha>0}\alpha(\phi_0)^{\chi_h}, \tag{208}$$

up to a normalization constant $\mathcal{N}$. The zero-mode integral is a multiple of the Abelian gauge theory except for the Vandermonde-type determinant $\prod_{\alpha>0}\alpha(\phi_0)^{\chi_h}$. This phenomenon is the same as occurs in continuum field theory localization and is called “diagonalization” or “Abelianization” (for a review see Ref. [61].) This integral measure has the $U(1)_A$ anomaly

$$\begin{aligned}&\prod_{i=1}^N d\phi^i_0 d\bar{\phi}^i_0\left(\prod_{I=1}^{2h}d\lambda_0^{i,2h-I+1}\right)d\,\chi^i_0 d\eta^i_0\prod_{\alpha>0}\alpha(\phi_0)^{\chi_h}\\ &\quad\to e^{iN^2\chi_h\theta_A}\prod_{i=1}^N d\phi^i_0 d\bar{\phi}^i_0\left(\prod_{I=1}^{2h}d\lambda_0^{i,2h-I+1}\right)d\,\chi^i_0 d\eta^i_0\prod_{\alpha>0}\alpha(\phi_0)^{\chi_h},\end{aligned} \tag{209}$$

as expected.

Due to the existence of the fermion zero modes the partition function itself is ill-defined, so we need to insert an operator which compensates for the fermionic zero modes. As mentioned above, the path integral reduces to multiple integrals of the Abelian ones, so we can compensate for the fermionic zero modes by inserting the compensator discussed in Sect. 5.3 for each Cartan part. However, it seems to be difficult to construct a compensator that is invariant under the non-Abelian gauge group and supersymmetric (Q-closed) prior to the Abelianization. We leave the construction of the complete compensator in non-Abelian gauge theory as a future problem.

7. Conclusion and discussion

In this paper, the properties of the discretized two-dimensional supersymmetric gauge theory (the generalized Sugino model) given in Ref. [52] have been studied analytically using the techniques of graph theory.

From a graph theory point of view, the model is defined on a two-dimensional graph and its dual graph, and the action can be efficiently described using the so-called incidence matrix L and the dual incidence matrix $\check{L}$.

The incidence and dual incidence matrices respectively map from a vector on the vertices to a vector on the edges and form a vector on the faces to a vector on the edges, and obey the property that $L\check{L}^{\mathrm{T}} = 0$. Therefore, if we consider the vectors on the vertices, edges, and faces as analogs of 0-forms, 1-forms, and 2-forms, respectively, we can regard L and $\check{L}^{\mathrm{T}}$ as the exterior derivatives, and L^{T} and $\check{L}$ as their dual. The cohomology can be defined using L and $\check{L}$, and a parallel argument to Hodge's theorem on the Riemann surfaces can be developed on the graphs. In particular, we found that the structure of the kernel of L and $\check{L}$ is completely determined by the topology of the graph.

We used the properties of these matrices to examine the generalized Sugino model with gauge group $U(1)$ and found that the number of fermion zero modes depends on the topology of the graph. Since these zero modes make the partition function ill-defined, it is necessary to insert an appropriate operator including zero modes in the background. We proposed a mass term for the fermions so that this operation is done automatically. We confirmed that the introduction of this mass term regularizes the Dirac matrix and makes the theory itself well-defined. We also derived anomalous WT identities on the graph corresponding to the classical global $U(1)$ symmetry, which is broken quantum mechanically unless the topology of the graph is the torus. In the continuous theory, this anomaly appears as the scalar curvature in the WT identity. On the other hand, in the theory on a graph, a quantity related to the degrees of the vertices and faces arises instead of the scalar curvature. This corresponds to the fact that the scalar curvature of a two-dimensional surface is given by the deficit angle.

We examined the generalized Sugino model from the viewpoint of topological field theory by restricting the physical quantity to Q-cohomology. We used the so-called localization technique to compute the expected value of a general Q-closed operator. As a result of localization, the vev can be expressed in terms of the usual integration by the zero modes. In that case, unless the operator contains all the fermion zero modes, the vev trivially vanishes. We constructed Q-invariant operators (compensators) that cancel out the fermion zero modes, and gave a prescription for computing the vev for nontrivial values. The compensators introduced here regularize the theory properly.

We also extended the graph-theoretic description to the non-Abelian theory. Reflecting the non-commutativity of gauge groups, the incidence and dual incidence matrices are transformed to be covariant differences instead of ordinary differences. This transformation eliminates the orthogonality of the incidence and dual incidence matrices unless all the plaquette variables are unity ($P^f = 1$), and the fermion zero modes that appeared in the Abelian theory are lifted in most configurations. Therefore, in most configurations the Dirac matrix is regular and the inverse exists. However, the situation is different around the saddle points of the Q-transformation. Using the localization technique with an appropriate gauge fixing, the non-Abelian generalized Sugino model can be effectively reduced to an Abelian theory. As a result, the evaluation of the partition function is completely parallel to the calculation of that of the Abelian theory, and the fermion zero modes arising at the saddle points make an important contribution. In particular, it is confirmed that the partition function becomes ill-defined unless these fermion zero modes on the saddle points are properly treated.

The fact that the non-Abelian generalized Sugino model is also affected by the fermion zero modes is quite important when carrying out numerical simulations. As mentioned above, the fermion zero modes appear only on the saddle points of the Q-transformation and thus the Dirac matrix is regular in almost all configurations. Therefore, the numerical simulation proceeds even without any special treatment for the zero modes. However, since the saddle points of the Q-transformation are part of the classical configurations, the zero modes would affect the computation, especially in the region close to the continuum limit, and there is a possibility that reliable results cannot be obtained. This conclusion holds even in the case of a torus background where the anomaly is canceled because the fermion zero modes still exist at the saddle points.

In the case of the torus, the fermion zero modes are completely lifted up by imposing the anti-periodic boundary condition in the temporal direction to the fermions. Therefore, the numerical simulations for a system with finite temperature are expected to work well. All the simulations imposing anti-periodic boundary conditions for the fermions in the temporal direction have been successfully carried out [30–35].

On the other hand, it was reported in Ref. [32] that numerical calculations did not yield the expected results for two-point functions in the continuum limit,[8] while it was reported in Ref. [35] that the vevs of Yukawa terms consistently degenerate in the continuum limit.

At first glance, it seems that the simulation will not work in the presence of fermion zero modes, but the situation is slightly more complicated. The point is that the theory is expected to have (at least) two phases: the phase where the eigenvalues of the scalar field form a bound state, and the phase where they run freely [35]. In the numerical simulation, the flat directions of the scalar field are controlled by introducing a mass term, and thus the configurations are all in the phase with the bound state. On the other hand, the partition function in Eq. (208) is obtained by integrating out all the configurations including both phases. Therefore, although it is one of the possibilities, if the fermion zero modes are effectively lifted up in the phase with the bound state, the simulation would work well even if one takes the periodic boundary condition for the fermions. It will be interesting to check whether the situation changes if we deal with the fermion zero modes in an appropriate way.

It is only when the background is a torus that the boundary condition can eliminate all the fermion zero modes. This is because changing the boundary condition is equivalent to transforming $D = (L, \check{L})$. In the case of the torus D is a square matrix, so all zero modes will be eliminated if we transform it in such a way that the zero modes of L and $\check{L}$ are eliminated; imposing the anti-periodic boundary condition is an example of this kind of modification. On the other hand, in non-torus cases there are always zero modes no matter how much D is deformed since the rank of the rectangular matrix D is at most $\min(n_E, n_V + n_F)$. It is therefore a peculiarity of the torus that the zero modes can be dealt with just by considering the finite temperature.

[8] See also Ref. [36], where the WT identity is analytically examined using a “semi-perturbative” treatment.

In the non-toric cases we have to insert some corrections to the diagonal blocks of $\not{D}$ to eliminate all the fermion zero modes. This is equivalent to introducing a mass term to the fermions, and Eq. (106) is an example of this kind of modification. In the case of non-Abelian theories it is necessary to introduce such a mass term that appropriately lifts the zero modes arising on the Q-fixed points without breaking the gauge symmetry and respecting the Q symmetry if possible. For the zero modes of η and χ, we can simply extend the compensator in Eq. (150) as

$$Q\,\mathrm{tr}\big(\chi_f \bar{\mathcal{W}}'(\bar{\phi}^f)\big). \tag{210}$$

For the zero modes of λ, however, it is still an open problem to construct such an operator that is Q-closed (not Q-exact) and includes bi-linear terms of λ like Eq. (157). Instead, Q-exact operators like

$$Q\,\mathrm{tr}\left(\lambda_l P_f\right) \tag{211}$$

may work. It will also be interesting to analyze the properties of non-Abelian compensators.

One problem that has not yet been solved in previous studies is the introduction of matter fields. In supersymmetric gauge theories, in order to introduce the matter field as a chiral multiplet, it is essential to consider chiral fermions.

Chiral fermions have been constructed on the regular square lattice by various methods, but how to construct chiral fermions on a discrete space arbitrarily partitioned by a graph is completely unknown. However, in this paper we have clarified that the incidence matrix in graph theory has a deep connection with the Dirac operator, so it seems possible to define chiral fermions using graph theory. We could use graph theory to introduce chiral fermions on discrete spaces, to construct supersymmetric gauge theories including matter fields, and to analyze and understand chiral anomalies induced by chiral fermions. These are also important future issues.

Once the introduction of the matter field is achieved, the interaction with the gauge field also allows the construction of solitons such as vortices on the discretized Riemann surface. At present, the construction of solitons on the graph is a novel problem. It will also be very interesting to understand the non-perturbative effects by such solitons in supersymmetric gauge theories on the graph.

As mentioned in the introduction, the continuum limit of the generalized Sugino model is a topologically twisted $\mathcal{N} = (2, 2)$ supersymmetric gauge theory, which is a theory on the Riemann surface with a $U(1)_A$ background field balanced with the spin connection of the background space-time, and the fermions behave as fields with integer spins. Interestingly, this property is similar to the Kähler–Dirac fermion. In fact, it is argued in Refs. [62,63] that systems with a Kähler–Dirac fermion have an anomaly proportional to the background Euler number as well. These approaches would be compatible with lattice gravity, which realizes gravity via a random triangulation. For example, in the formulation given in Ref. [64], it is essential to place the gauge field on the edge of the triangulation, and the spin connection on the dual edge. It is remarkable that in this formulation the action of gravity is written in terms of the deficit angle of the dual plaquette, whereas the anomaly in the local WT identities appears as the deficit angle as well. It will be interesting to consider lattice gravity from the viewpoint of graph theory. In particular, it is suggestive that the construction of the discretized theory with supersymmetry is possible only when the spin connection and the background gauge field are properly balanced. Through research in this direction we expect to obtain new insights from graph theory for lattice gravity in higher dimensions [64–66].

Acknowledgments

We would like to thank S. Kamata and T. Misumi for useful discussions in the early stages of this work. We would like to thank N. Kawamoto for useful discussions at Hokkaido University and for showing us stimulating references. S.M. would like to thank M. Hanada and D. Kadoh for useful discussions. This work is supported in part by Grants-in-Aid for Scientific Research (KAKENHI) (C) nos. 17K05422 (K. O.) and 20K03934 (S. M.). Part of this work is motivated by the results of numerical simulations carried out on the Oakforest-PACS computational system provided by Tokyo University through the HPCI System Research Project (Project ID: hp200052).

Funding

Open Access funding: SCOAP^3.

Appendix A. Examples of graph data

In this appendix we give concrete examples of the graph data and objects, and check some properties. We also give plaquette variables on each face and covariantized version of the (dual) incidence matrix in non-Abelian gauge theory.

A1. Tetrahedron

A directed graph associated with a tetrahedron is shown in Fig. A1. There are four vertices, labeled by $V(\Gamma) = \{v_1, v_2, v_3, v_4\}$. The directed connectivity for the six edges is given by $E(\Gamma) = \{e_1, e_2, e_3, e_4, e_5, e_6\} = \{v_1 \to v_2, v_1 \to v_3, v_1 \to v_4, v_2 \to v_3, v_3 \to v_4, v_4 \to v_2\}$.

For this directed graph, the incidence matrix is given by

$$L = \begin{pmatrix} -1 & 1 & 0 & 0 \\ -1 & 0 & 1 & 0 \\ -1 & 0 & 0 & 1 \\ 0 & -1 & 1 & 0 \\ 0 & 0 & -1 & 1 \\ 0 & 1 & 0 & -1 \end{pmatrix}. \tag{A1}$$

We can construct the Laplacian matrix for the vertex from the incidence matrix:

$$\Delta_V = L^{\mathrm{T}} L = \begin{pmatrix} 3 & -1 & -1 & -1 \\ -1 & 3 & -1 & -1 \\ -1 & -1 & 3 & -1 \\ -1 & -1 & -1 & 3 \end{pmatrix}. \tag{A2}$$

Then, the adjacency matrix becomes

$$K = \begin{pmatrix} 0 & 1 & 1 & 1 \\ 1 & 0 & 1 & 1 \\ 1 & 1 & 0 & 1 \\ 1 & 1 & 1 & 0 \end{pmatrix}. \tag{A3}$$

The vertex Laplacian has the eigenvalues $\{4, 4, 4, 0\}$, which contain one zero.

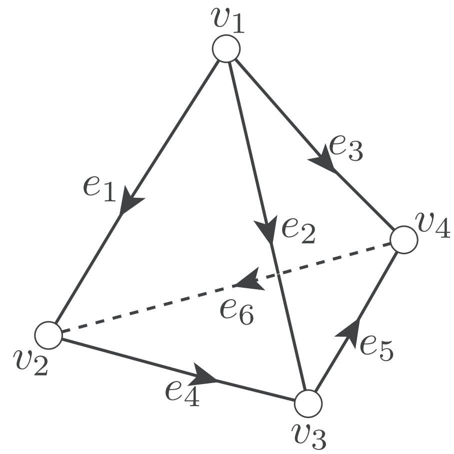

Fig. A1. A directed graph for a tetrahedron. There are four vertices and six directed edges.

The four faces are defined by $f_1 = \{e_1, e_4, \bar{e}_2\}$, $f_2 = \{e_2, e_5, \bar{e}_3\}$, $f_3 = \{e_3, e_6, \bar{e}_1\}$, and $f_3 = \{\bar{e}_4, \bar{e}_6, \bar{e}_5\}$. The dual incidence matrix is then given by

$$\check{L} = \begin{pmatrix} 1 & 0 & -1 & 0 \\ -1 & 1 & 0 & 0 \\ 0 & -1 & 1 & 0 \\ 1 & 0 & 0 & -1 \\ 0 & 1 & 0 & -1 \\ 0 & 0 & 1 & -1 \end{pmatrix}. \tag{A4}$$

We can see that $L^{\mathrm{T}}\check{L} = \check{L}^{\mathrm{T}}L = 0$.

Using the dual incidence matrix we can construct the Laplacian for the face and edges as

$$\Delta_F = \check{L}^{\mathrm{T}}\check{L} = \begin{pmatrix} 3 & -1 & -1 & -1 \\ -1 & 3 & -1 & -1 \\ -1 & -1 & 3 & -1 \\ -1 & -1 & -1 & 3 \end{pmatrix},$$

$$\Delta_E = LL^{\mathrm{T}} + \check{L}\check{L}^{\mathrm{T}} = \begin{pmatrix} 4 & 0 & 0 & 0 & 0 & 0 \\ 0 & 4 & 0 & 0 & 0 & 0 \\ 0 & 0 & 4 & 0 & 0 & 0 \\ 0 & 0 & 0 & 4 & 0 & 0 \\ 0 & 0 & 0 & 0 & 4 & 0 \\ 0 & 0 & 0 & 0 & 0 & 4 \end{pmatrix}, \tag{A5}$$

which have the eigenvalues $\{4, 4, 4, 0\}$ and $\{4, 4, 4, 4, 4, 4\}$, respectively.

A non-Abelian generalization for the incidence matrix acting on the adjoint representation is given by

$$L_U = \begin{pmatrix} -1 & U^1 \cdot U^{1\dagger} & 0 & 0 \\ -1 & 0 & U^2 \cdot U^{2\dagger} & 0 \\ -1 & 0 & 0 & U^3 \cdot U^{3\dagger} \\ 0 & -1 & U^4 \cdot U^{4\dagger} & 0 \\ 0 & 0 & -1 & U^5 \cdot U^{5\dagger} \\ 0 & U^6 \cdot U^{6\dagger} & 0 & -1 \end{pmatrix}, \tag{A6}$$

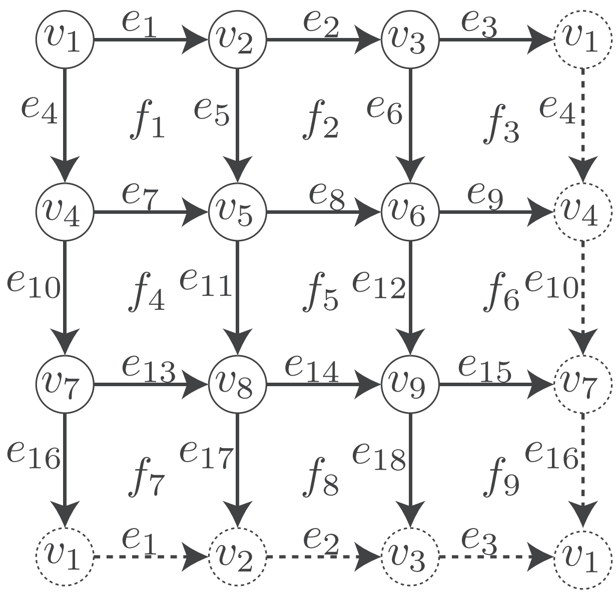

Fig. A2. A directed graph for a 3 × 3 torus. There are 9 vertices, 9 faces, and 18 directed edges.

where $\cdot$ stands for an insertion position of matrices in the adjoint representation when this covariant incidence matrix acts from the right, for example

$$(X \cdot Y)A = XAY. \tag{A7}$$

The conjugate of the dual incidence matrix is derived from the four plaquette variables

$$P^1 = U^1 U^4 U^{2\dagger}, \qquad P^2 = U^2 U^5 U^{3\dagger}, \qquad P^3 = U^3 U^6 U^{1\dagger}, \qquad P^4 = U^{4\dagger} U^{6\dagger} U^{5\dagger}. \tag{A8}$$

It becomes

$$\check{L}_U^\dagger = \begin{pmatrix} \cdot P^1 & -P^1 \cdot & 0 & U^1 \cdot U^{1\dagger} P^1 & 0 & 0 \\ 0 & \cdot P^2 & -P^2 \cdot & 0 & U^2 \cdot U^{2\dagger} P^2 & 0 \\ -P^3 \cdot & 0 & \cdot P^3 & 0 & 0 & U^3 \cdot U^{3\dagger} P^3 \\ 0 & 0 & 0 & -U^{4\dagger} \cdot U^4 P^4 & -P^4 \cdot & -P^4 U^5 \cdot U^{5\dagger} \end{pmatrix}. \tag{A9}$$

Then, we find that $L_U^\dagger \check{L}_U = \check{L}_U^\dagger L_U = 0$ if and only if $P^f = 1$.

We can also define the covariant Laplacians by

$$\Delta_U^V = L_U^\dagger L_U, \qquad \Delta_U^F = \check{L}_U^\dagger \check{L}_U, \qquad \Delta_U^E = L_U L_U^\dagger + \check{L}_U \check{L}_U^\dagger, \tag{A10}$$

which have the same eigenvalues as Δ_V, Δ_F, and Δ_E if and only if $P^f = 1$.

A2. Torus

A directed graph for a torus is depicted in Fig. A2. The torus is divided into 3 × 3 square faces (nine faces in total) and the associated graph has a periodicity for two directions.

We first provide the covariant incidence matrix for this graph. We can immediately reproduce the usual incidence matrix by setting $U^e = 1$ for all:

$$
L_U = \left(\begin{array}{cccccccccc}
-1 & U^1 \cdot U^{1\dagger} & 0 & 0 & 0 & 0 & 0 & 0 & 0 & \\
0 & -1 & U^2 \cdot U^{2\dagger} & 0 & 0 & 0 & 0 & 0 & 0 & \\
U^3 \cdot U^{3\dagger} & 0 & -1 & 0 & 0 & 0 & 0 & 0 & 0 & \\
-1 & 0 & 0 & U^4 \cdot U^{4\dagger} & 0 & 0 & 0 & 0 & 0 & \\
0 & -1 & 0 & 0 & U^5 \cdot U^{5\dagger} & 0 & 0 & 0 & 0 & \\
0 & 0 & -1 & 0 & 0 & U^6 \cdot U^{6\dagger} & 0 & 0 & 0 & \\
0 & 0 & 0 & -1 & U^7 \cdot U^{7\dagger} & 0 & 0 & 0 & 0 & \\
0 & 0 & 0 & 0 & -1 & U^8 \cdot U^{8\dagger} & 0 & 0 & 0 & \\
0 & 0 & 0 & U^9 \cdot U^{9\dagger} & 0 & -1 & 0 & 0 & 0 & \\
0 & 0 & 0 & -1 & 0 & 0 & U^{10} \cdot U^{10\dagger} & 0 & 0 & s \\
0 & 0 & 0 & 0 & -1 & 0 & 0 & U^{11} \cdot U^{11\dagger} & 0 & \\
0 & 0 & 0 & 0 & 0 & -1 & 0 & 0 & U^{12} \cdot U^{12\dagger} & \\
0 & 0 & 0 & 0 & 0 & 0 & -1 & U^{13} \cdot U^{13\dagger} & 0 & \\
0 & 0 & 0 & 0 & 0 & 0 & 0 & -1 & U^{14} \cdot U^{14\dagger} & \\
0 & 0 & 0 & 0 & 0 & 0 & U^{15} \cdot U^{15\dagger} & 0 & -1 & \\
U^{16} \cdot U^{16\dagger} & 0 & 0 & 0 & 0 & 0 & -1 & 0 & 0 & \\
0 & U^{17} \cdot U^{17\dagger} & 0 & 0 & 0 & 0 & 0 & -1 & 0 & \\
0 & 0 & U^{18} \cdot U^{18\dagger} & 0 & 0 & 0 & 0 & 0 & -1 &
\end{array}\right). \tag{A11}
$$

The Laplacian matrix on the vertex is

$$
\Delta_V = \begin{pmatrix}
4 & -1 & -1 & -1 & 0 & 0 & -1 & 0 & 0 \\
-1 & 4 & -1 & 0 & -1 & 0 & 0 & -1 & 0 \\
-1 & -1 & 4 & 0 & 0 & -1 & 0 & 0 & -1 \\
-1 & 0 & 0 & 4 & -1 & -1 & -1 & 0 & 0 \\
0 & -1 & 0 & -1 & 4 & -1 & 0 & -1 & 0 \\
0 & 0 & -1 & -1 & -1 & 4 & 0 & 0 & -1 \\
-1 & 0 & 0 & -1 & 0 & 0 & 4 & -1 & -1 \\
0 & -1 & 0 & 0 & -1 & 0 & -1 & 4 & -1 \\
0 & 0 & -1 & 0 & 0 & -1 & -1 & -1 & 4
\end{pmatrix}, \tag{A12}
$$

which has the eigenvalues $\{6, 6, 6, 6, 3, 3, 3, 3, 0\}$.

The covariant dual incidence matrix is made from the plaquette variables, but it is a huge matrix that does not fit here. To display it we give the incidence matrix by setting $U^e = 1$:

$$
\check{L}^{\mathrm{T}} = \begin{pmatrix}
-1 & 0 & 0 & 1 & -1 & 0 & 1 & 0 & 0 & 0 & 0 & 0 & 0 & 0 & 0 & 0 & 0 & 0 \\
0 & -1 & 0 & 0 & 1 & -1 & 0 & 1 & 0 & 0 & 0 & 0 & 0 & 0 & 0 & 0 & 0 & 0 \\
0 & 0 & -1 & -1 & 0 & 1 & 0 & 0 & 1 & 0 & 0 & 0 & 0 & 0 & 0 & 0 & 0 & 0 \\
0 & 0 & 0 & 0 & 0 & 0 & -1 & 0 & 0 & 1 & -1 & 0 & 1 & 0 & 0 & 0 & 0 & 0 \\
0 & 0 & 0 & 0 & 0 & 0 & 0 & -1 & 0 & 0 & 1 & -1 & 0 & 1 & 0 & 0 & 0 & 0 \\
0 & 0 & 0 & 0 & 0 & 0 & 0 & 0 & -1 & -1 & 0 & 1 & 0 & 0 & 1 & 0 & 0 & 0 \\
1 & 0 & 0 & 0 & 0 & 0 & 0 & 0 & 0 & 0 & 0 & 0 & -1 & 0 & 0 & 1 & -1 & 0 \\
0 & 1 & 0 & 0 & 0 & 0 & 0 & 0 & 0 & 0 & 0 & 0 & 0 & -1 & 0 & 0 & 1 & -1 \\
0 & 0 & 1 & 0 & 0 & 0 & 0 & 0 & 0 & 0 & 0 & 0 & 0 & 0 & -1 & -1 & 0 & 1
\end{pmatrix}. \tag{A13}
$$

The Laplacian matrix on the face Δ_F is the same as Δ_V in Eq. (A12). The Laplacian matrix on the edge is given by

$$\Delta_E = \begin{pmatrix} 4 & -1 & -1 & 0 & 0 & 0 & -1 & 0 & 0 & 0 & 0 & 0 & -1 & 0 & 0 & 0 & 0 & 0 \\ -1 & 4 & -1 & 0 & 0 & 0 & 0 & -1 & 0 & 0 & 0 & 0 & 0 & -1 & 0 & 0 & 0 & 0 \\ -1 & -1 & 4 & 0 & 0 & 0 & 0 & 0 & -1 & 0 & 0 & 0 & 0 & 0 & -1 & 0 & 0 & 0 \\ 0 & 0 & 0 & 4 & -1 & -1 & 0 & 0 & 0 & -1 & 0 & 0 & 0 & 0 & 0 & -1 & 0 & 0 \\ 0 & 0 & 0 & -1 & 4 & -1 & 0 & 0 & 0 & 0 & -1 & 0 & 0 & 0 & 0 & 0 & -1 & 0 \\ 0 & 0 & 0 & -1 & -1 & 4 & 0 & 0 & 0 & 0 & 0 & -1 & 0 & 0 & 0 & 0 & 0 & -1 \\ -1 & 0 & 0 & 0 & 0 & 0 & 4 & -1 & -1 & 0 & 0 & 0 & -1 & 0 & 0 & 0 & 0 & 0 \\ 0 & -1 & 0 & 0 & 0 & 0 & -1 & 4 & -1 & 0 & 0 & 0 & 0 & -1 & 0 & 0 & 0 & 0 \\ 0 & 0 & -1 & 0 & 0 & 0 & -1 & -1 & 4 & 0 & 0 & 0 & 0 & 0 & -1 & 0 & 0 & 0 \\ 0 & 0 & 0 & -1 & 0 & 0 & 0 & 0 & 0 & 4 & -1 & -1 & 0 & 0 & 0 & -1 & 0 & 0 \\ 0 & 0 & 0 & 0 & -1 & 0 & 0 & 0 & 0 & -1 & 4 & -1 & 0 & 0 & 0 & 0 & -1 & 0 \\ 0 & 0 & 0 & 0 & 0 & -1 & 0 & 0 & 0 & -1 & -1 & 4 & 0 & 0 & 0 & 0 & 0 & -1 \\ -1 & 0 & 0 & 0 & 0 & 0 & -1 & 0 & 0 & 0 & 0 & 0 & 4 & -1 & -1 & 0 & 0 & 0 \\ 0 & -1 & 0 & 0 & 0 & 0 & 0 & -1 & 0 & 0 & 0 & 0 & -1 & 4 & -1 & 0 & 0 & 0 \\ 0 & 0 & -1 & 0 & 0 & 0 & 0 & 0 & -1 & 0 & 0 & 0 & -1 & -1 & 4 & 0 & 0 & 0 \\ 0 & 0 & 0 & -1 & 0 & 0 & 0 & 0 & 0 & -1 & 0 & 0 & 0 & 0 & 0 & 4 & -1 & -1 \\ 0 & 0 & 0 & 0 & -1 & 0 & 0 & 0 & 0 & 0 & -1 & 0 & 0 & 0 & 0 & -1 & 4 & -1 \\ 0 & 0 & 0 & 0 & 0 & -1 & 0 & 0 & 0 & 0 & 0 & -1 & 0 & 0 & 0 & -1 & -1 & 4 \end{pmatrix}, \tag{A14}$$

which has the eigenvalues $\{6, 6, 6, 6, 6, 6, 6, 6, 3, 3, 3, 3, 3, 3, 3, 3, 0, 0\}$.

We can also show the orthogonality $L_U^\dagger \check{L}_U = \check{L}_U^\dagger L_U = 0$ if and only if $P^f = 1$ explicitly.

Appendix B. The Cartan–Weyl basis and properties

We denote the generators in the Cartan subalgebra $\mathfrak{u}(N)$ by H_i ($i = 1, \ldots, N$) and the root vectors (Weyl generators) by E_α. These generators obey the commutation relations

$$[\mathrm{H}_i, \mathrm{H}_j] = 0, \quad [\mathrm{H}_i, \mathrm{E}_{\pm\alpha}] = \pm\alpha_i \mathrm{E}_{\pm\alpha}, \quad [\mathrm{E}_\alpha, \mathrm{E}_{-\alpha}] = \sum_{i=1}^{N} \alpha_i \mathrm{H}_i, \quad [\mathrm{E}_\alpha, \mathrm{E}_\beta] = N_{\alpha,\beta} \mathrm{E}_{\alpha+\beta}, \tag{B1}$$

and have the properties

$$\mathrm{E}_\alpha^\dagger = \mathrm{E}_{-\alpha}, \qquad \mathrm{Tr}\, \mathrm{E}_\alpha \mathrm{E}_\beta = \delta_{\alpha+\beta,0}, \qquad \mathrm{Tr}\, \mathrm{H}_i \mathrm{H}_j = \sum_\alpha \alpha_i \alpha_j = \delta_{ij}. \tag{B2}$$

Any adjoint representation of the $U(N)$ group (generators of the Lie algebra) can be expanded by

$$X = \sum_{i=1}^{N} x^i \mathrm{H}_i + \sum_\alpha x^\alpha \mathrm{E}_\alpha. \tag{B3}$$

We use these conventions in the manuscript.

References

[1] J. M. Maldacena, Adv. Theor. Math. Phys.; **2**, 231 (1998).
[2] E. Witten, Adv. Theor. Math. Phys.; **2**, 253 (1998).
[3] S. S. Gubser, I. R. Klebanov, and A. M. Polyakov, Phys. Lett. B; **428**, 105 (1998).
[4] F. Sugino, J. High Energy Phys. **01**, 015 (2004).
[5] F. Sugino, J. High Energy Phys. **03**, 067 (2004).

[6] F. Sugino, J. High Energy Phys. **01**, 016 (2005).
[7] F. Sugino, Phys. Lett. B **635**, 218 (2006).
[8] F. Sugino, Nucl. Phys. B **808**, 292 (2009).
[9] Y. Kikukawa and F. Sugino, Nucl. Phys. B **819**, 76 (2009).
[10] D. B. Kaplan, E. Katz, and M. Unsal, J. High Energy Phys. **05**, 037 (2003).
[11] A. G. Cohen, D. B. Kaplan, E. Katz, and M. Unsal, J. High Energy Phys. **08**, 024 (2003).
[12] A. G. Cohen, D. B. Kaplan, E. Katz, and M. Unsal, J. High Energy Phys. **12**, 031 (2003).
[13] D. B. Kaplan and M. Unsal, J. High Energy Phys. **09**, 042 (2005).
[14] A. D'Adda, I. Kanamori, N. Kawamoto, and K. Nagata, Nucl. Phys. B **707**, 100 (2005).
[15] A. D'Adda, I. Kanamori, N. Kawamoto, and K. Nagata, Phys. Lett. B **633**, 645 (2006).
[16] A. D'Adda, I. Kanamori, N. Kawamoto, and K. Nagata, Nucl. Phys. B **798**, 168 (2008).
[17] M. G. Endres and D. B. Kaplan, J. High Energy Phys. **10**, 076 (2006).
[18] J. Giedt, arXiv:hep-lat/0605004 [Search inSPIRE].
[19] S. Matsuura, J. High Energy Phys. **07**, 127 (2008).
[20] S. Catterall, J. High Energy Phys. **05**, 038 (2003).
[21] A. Joseph, J. High Energy Phys. **09**, 046 (2013).
[22] S. Catterall, J. High Energy Phys. **01**, 048 (2008).
[23] M. Unsal, J. High Energy Phys. **11**, 013 (2005).
[24] M. Unsal, J. High Energy Phys. **10**, 089 (2006).
[25] T. Takimi, J. High Energy Phys. **07**, 010 (2007).
[26] P. H. Damgaard and S. Matsuura, J. High Energy Phys. **08**, 087 (2007).
[27] P. H. Damgaard and S. Matsuura, J. High Energy Phys. **09**, 097 (2007).
[28] S. Catterall, J. High Energy Phys. **03**, 032 (2006).
[29] H. Suzuki, J. High Energy Phys. **09**, 052 (2007).
[30] I. Kanamori, H. Suzuki, and F. Sugino, Phys. Rev. D **77**, 091502 (2008).
[31] I. Kanamori, F. Sugino, and H. Suzuki, Prog. Theor. Phys. **119**, 797 (2008).
[32] I. Kanamori and H. Suzuki, Nucl. Phys. B **811**, 420 (2009).
[33] I. Kanamori and H. Suzuki, Phys. Lett. B **672**, 307 (2009).
[34] I. Kanamori, Phys. Rev. D **79**, 115015 (2009).
[35] M. Hanada and I. Kanamori, Phys. Rev. D **80**, 065014 (2009).
[36] D. Kadoh and H. Suzuki, Phys. Lett. B **682**, 466 (2010).
[37] S. Catterall, J. High Energy Phys. **01**, 040 (2009).
[38] S. Catterall, R. Galvez, A. Joseph, and D. Mehta, J. High Energy Phys. **01**, 108 (2012).
[39] S. Catterall, P. H. Damgaard, T. Degrand, R. Galvez, and D. Mehta, J. High Energy Phys. **11**, 072 (2012).
[40] S. Catterall, D. Schaich, P. H. Damgaard, T. DeGrand, and J. Giedt, Phys. Rev. D **90**, 065013 (2014).
[41] E. Giguère and D. Kadoh, J. High Energy Phys. **05**, 082 (2015).
[42] S. Catterall, R. G. Jha, and A. Joseph, Phys. Rev. D **97**, 054504 (2018).
[43] D. August, M. Steinhauser, B. H. Wellegehausen, and A. Wipf, J. High Energy Phys. **01**, 099 (2019).
[44] D. B. Kaplan, Nucl. Phys. B Proc. Suppl. **129**, 109 (2004).
[45] J. Giedt, Int. J. Mod. Phys. A **21**, 3039 (2006).
[46] S. Catterall, D. B. Kaplan, and M. Unsal, Phys. Rept. **484**, 71 (2009).
[47] A. Joseph, Int. J. Mod. Phys. A **26**, 5057 (2011).
[48] F. Sugino, Int. J. Mod. Phys. Conf. Ser. **21**, 22 (2013).
[49] G. Bergner and S. Catterall, Int. J. Mod. Phys. A **31**, 1643005 (2016).
[50] S. Matsuura and F. Sugino, J. High Energy Phys. **04**, 088 (2014).
[51] M. Hanada, D. Kadoh, S. Matsuura, and F. Sugino, Nucl. Phys. B **929**, 266 (2018).
[52] S. Matsuura, T. Misumi, and K. Ohta, Prog. Theor. Exp. Phys. **2014**, 123B01 (2014).
[53] S. Matsuura, T. Misumi, and K. Ohta, Prog. Theor. Exp. Phys. **2015**, 033B07 (2015).
[54] S. Kamata, S. Matsuura, T. Misumi, and K. Ohta, Prog. Theor. Exp. Phys. **2016**, 123B01 (2016).
[55] R. B. Bapat, Graphs and Matrices, **Universitext**, Second Edition, Springer (2014). 10.1007/978-1-4471-6569-9.
[56] N. Kan and K. Shiraishi, J. Math. Phys. **46**, 112301 (2005).
[57] N. Kan, K. Kobayashi, and K. Shiraishi, Phys. Rev. D **80**, 045005 (2009).
[58] N. Kan, K. Kobayashi, and K. Shiraishi, J. Phys. A **46**, 365401 (2013).

[59] K. Ohta and N. Sakai, Prog. Theor. Exp. Phys. **2021**, 033B02 (2021).
[60] K. Ohta and N. Sakai, Prog. Theor. Exp. Phys. **2019**, 043B01 (2019).
[61] M. Blau and G. Thompson, J. Math. Phys. **36**, 2192 (1995).
[62] S. Catterall, J. Laiho, and J. Unmuth-Yockey, J. High Energy Phys. **10**, 013 (2018).
[63] N. Butt, S. Catterall, A. Pradhan, and G. C. Toga, Phys. Rev. D **104**, 094504 (2021).
[64] N. Kawamoto and H. B. Nielsen, Phys. Rev. D **43**, 1150 (1991).
[65] N. Kawamoto, N. Sato, and Y. Uchida, Nucl. Phys. B **574**, 809 (2000).
[66] N. Kawamoto, H. B. Nielsen, and N. Sato, Nucl. Phys. B **555**, 629 (1999).